CALIFORNIA
ENERGY COMMISSION

Energy Research and Development Division

FINAL PROJECT REPORT

Demonstration of Community-Scale Low-Cost, Highly Efficient Photovoltaic and Energy Management System

Gavin Newsom, Governor

September 2022 | CEC-500-2022-006

PREPARED BY:

Primary Authors:
Joseph Lacap, Masoud Rahman, Jae Wan Park

Green Technology Laboratory at University of California, Davis
1 Shields Ave
Davis, CA 95616
(530) 754-9401
https://research.engineering.ucdavis.edu/greentech/

Contract Number: EPC-14-085

PREPARED FOR:
California Energy Commission

Abolghasem Edalati
Project Manager

Jonah Steinbuck, Ph.D
Office Manager
ENERGY GENERATION RESEARCH OFFICE

Laurie ten Hope
Deputy Director
ENERGY RESEARCH AND DEVELOPMENT DIVISION

Drew Bohan
Executive Director

ACKNOWLEDGEMENTS

The authors thank the following for their contributions to this project:

- The California Energy Commission for funding this work
- Abolghasem Edalati for helping to manage and resolve project’s outstanding issues
- Nissan USA, 4R Energy, and Sumitomo for providing the second-life electric vehicle batteries
- Dr. Masoud Rahman for work on design review, production quality control, project management, and research team coordinator
- Jonathon Schadt for setup, maintenance, support, and debugging of the plant information data servers.
- Lucas Beslow for data and performance analysis
- Alex Chew for engineering work on the battery system and construction of the battery system
- Vivian Tran for engineering work on the battery system, energy management system, and construction of the battery system
- Katherine Wikler for engineering work on the battery system and construction of the battery system
- Asad Rafiee for leading construction of the battery system
- Aliakbar Izadkhah for development of the communications software for the energy management system
- Jesse Kullar for integration of the energy management system with the plant information data server
- Nicolas C. Strauss for development of the solar forecasting model for the energy management system
- Peter Benoliel for managing laboratory safety during battery system construction, battery tacking and record keeping, and control engineering.
- Andrew Shoats, Areeb Mehmood, Carlos Urdampilleta, Jose Salinas, and Norberto Martinez for battery system construction
- Jacklyn Tran for engineering support
- Loan-Anh Nguyen for laboratory safety procedures during battery construction and coordination with university officials
- Chi Zhang for battery system assembly

PREFACE

The California Energy Commission's (CEC) Energy Research and Development Division supports energy research and development programs to spur innovation in energy efficiency, renewable energy and advanced clean generation, energy-related environmental protection, energy transmission and distribution and transportation.

In 2012, the Electric Program Investment Charge (EPIC) was established by the California Public Utilities Commission to fund public investments in research to create and advance new energy solutions, foster regional innovation and bring ideas from the lab to the marketplace. The CEC and the state's three largest investor-owned utilities—Pacific Gas and Electric Company, San Diego Gas & Electric Company and Southern California Edison Company—were selected to administer the EPIC funds and advance novel technologies, tools, and strategies that provide benefits to their electric ratepayers.

The CEC is committed to ensuring public participation in its research and development programs that promote greater reliability, lower costs, and increase safety for the California electric ratepayer and include:

- Providing societal benefits.
- Reducing greenhouse gas emission in the electricity sector at the lowest possible cost.
- Supporting California's loading order to meet energy needs first with energy efficiency and demand response, next with renewable energy (distributed generation and utility scale), and finally with clean, conventional electricity supply.
- Supporting low-emission vehicles and transportation.
- Providing economic development.
- Using ratepayer funds efficiently.

Demonstration of Community Scale Low Cost Highly Efficient PV and Energy Management System is the final report for the Demonstration of Community Scale Low Cost Highly Efficient PV and Energy Management System project (Contract Number: EPC-14-085) conducted by the Green Technology Laboratory at University of California, Davis. The information from this project contributes to the Energy Research and Development Division's EPIC Program.

For more information about the Energy Research and Development Division, please visit the CEC's research website (www.energy.ca.gov/research/) or contact the CEC at ERDD@energy.ca.gov.

ABSTRACT

The need for grid-connected energy storage will continue to grow due to the penetration of renewables and increasing demand for a secure and stable grid. Utilizing retired electric vehicle lithium-ion batteries (second-life lithium-ion batteries) is appealing to energy storage applications since they provide comparable performance at a reduced cost. This report outlines the design, construction, and benefits to California of a commercial scale microgrid at the Robert Mondavi Winery at the University of California, Davis. The microgrid consisted of 200 kilowatts of solar photovoltaics and 280 kilowatt-hours of energy storage supporting the load of two buildings. I energy storage system constructed under this project consisted of second-life Nissan LEAF battery modules to demonstrate the performance potential of second-life electric vehicle batteries for stationary energy storage.iiieducingearch team developed an energy management system to maximize onsite use of photovoltaic power and minimize peak-time energy demand while reducing the carbon footprint of the winery. The report discusses implementation challenges encountered during the project such as fire codes and component supply issues for microgrids. Benefits of this microgrid included energy savings, with up to 39 percent peak energy use reduced and $12,000 per year saved on electricity bills, iiieducinging the carbon footprint of the winery by 14,000 kilograms of carbon dioxide per year.

Keywords: Energy storage, second life, microgrid, reuse, lithium-ion, battery

Please use the following citation for this report:

Lacap, Joseph, Masoud Rahman, and Jae Wan Park. 2021. *Demonstration of Community-Scale Low-Cost Highly Efficient Photovoltaic and Energy Management System* . California Energy Commission. Publication Number: CEC-500-2022-006.

TABLE OF CONTENTS

Page

LIST OF FIGURES

Page

LIST OF TABLES

EXECUTIVE SUMMARY

Introduction

The intermittent nature of solar energy generation requires special attention when connecting to the grid. Critical issues include the grid instability of the distributed energy and imbalance between energy demand and production, especially during periods of over-generation. Although energy storage has the potential to serve multiple valuable functions in a microgrid setting, it is currently a very expensive resource because it is generally in the early stages of technology development. Renewable-based microgrids also require a reliable control system since they have insufficient inertia to dampen disturbances from distributed generation. Second-life lithium-ion batteries are appealing for energy storage system (ESS) applications since they provide comparable performance to new lithium-ion batteries, but at a reduced cost. Additionally, small scale battery systems provide a decentralized, scalable, and more responsive ESS solution, which supports the needs of the grid by performing demand response (DR) and dynamic peak shifting.

This project aimed to verify that second-life electric vehicle (EV) batteries could be used to reduce the high costs of energy storage for microgrids. The technology was demonstrated at the Brewery Winery and Food Science Building of the Robert Mondavi Institute (RMI) at the University of California (UC) Davis campus. California's wine and brewery market represents a significant market and if this concept is demonstrated successfully at this site, it is expected to be adopted elsewhere.

Project Purpose

The project developed and demonstrated a smart ESS system using retired EV batteries to store electricity generated by rooftop solar photovoltaic (PV) panels. The ESS provides a cost effective and efficient energy storage solution for a community scale grid with multiple renewable generation sources. The ESS acts as an energy buffer, storing power and shifting energy from distributed energy resources (DER) peak to grid energy consumption peak. Power was generated by new pre-commercial high performance solar PV panels. A commercial grade controller was developed to control the renewable energy sources and ESS system. Grid stability was further improved using a grid control Energy Management System (EMS) designed to mitigate grid instability.

The overall goals and objectives of this project were to demonstrate that a second-life ESS's operation could result in more than a 10 percent decrease in the daily average energy demand during peak times over a one-year period, as defined by the utility tariff, and that the system can be profitable by selling ancillary services to the California Independent System Operator's (California ISO) fast regulation market and participating in DR. It is designed to address the requirements of Assembly Bill 32, the California Global Warming Solutions Act, and general need for assured access to reliable sources of energy to provide the ratepayer benefits of greater electricity reliability and lower costs. With the support of the ESS and proper energy management control, the microgrid can be run at maximum renewable generation of up to 100 percent.

Project Approach

The RMI grid consists of the RMI-Brewery/Winery/Food Science Laboratory and Jess S. Jackson Sustainable Winery Building. The RMI-Brewery/Winery/Food Science Laboratory is a

Leadership in Energy and Environmental Design (LEED) platinum certified facility known as the greenest brewery in the world. Figure ES-1 shows the power feed diagram of RMI grid. It has one 800-kilowatt (kW) diesel generator and 120 kW solar PV. As part of this project, an additional 80 kW of high efficiency solar PV, and an ESS of 280 kilowatt-hour (kWh) capacity was added.

Figure ES-1: Robert Mondavi Institute Grid Layout

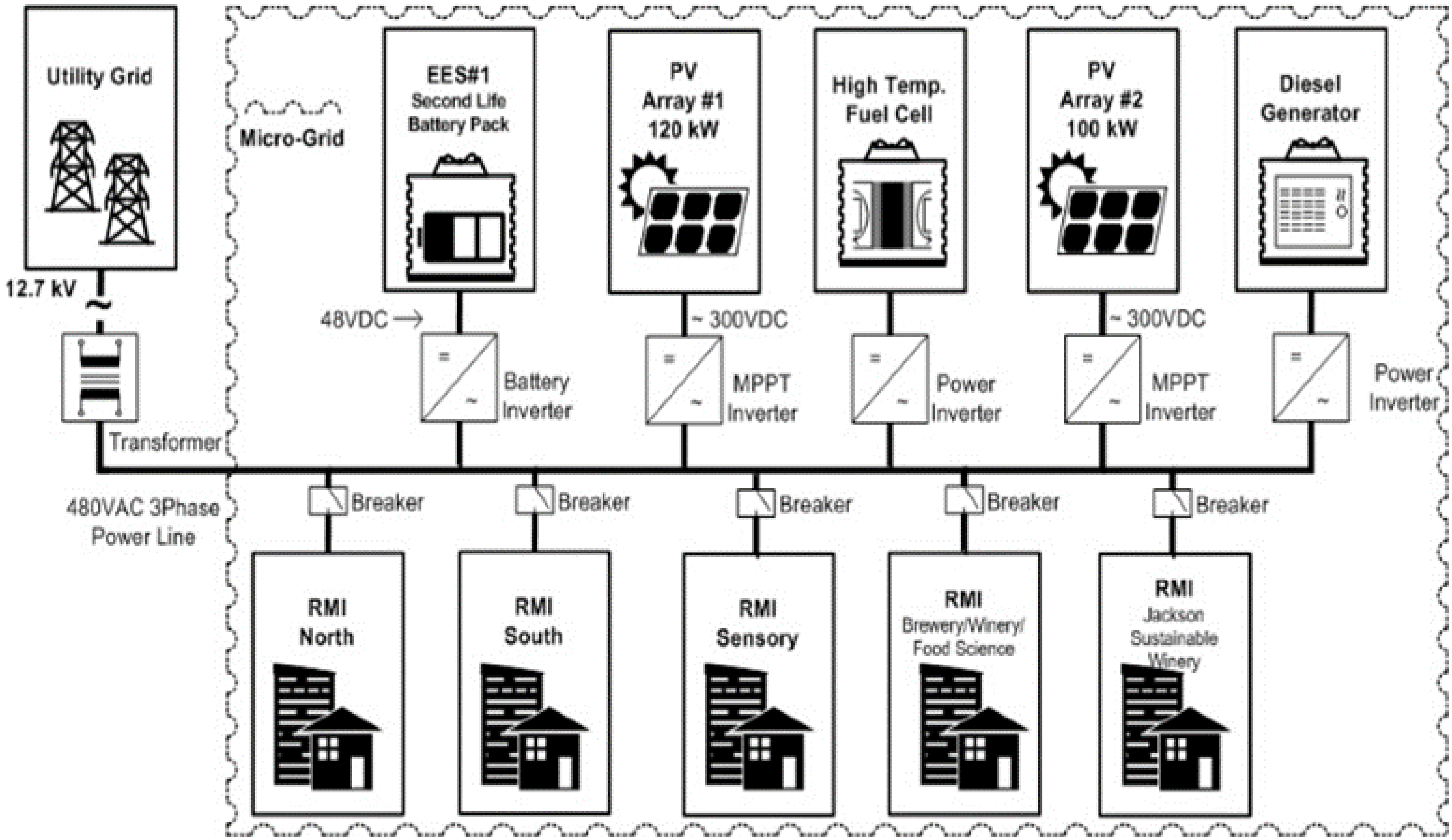

Source: UC Davis

The project team and key stakeholders included Professor Jae Wan Park, principal investigator; Jill Brigham, UC Davis project manager; Dr. Masoud Rahman, the laboratory manager for Professor Park's laboratory; Joseph Lacap, a Ph.D. candidate in Professor Park's laboratory; OSIsoft, provider of the data management and visualization system for the project as match funding, and UC Davis; provider of the host site for the project. Solexel was originally intended to supply precommercial solar panels for the microgrid, but due to economic conditions was unable to do so. In addition to these team members, a Technical Advisory Committee was also formed. This committee consisted of Brad Smith, General Manager at Nissan/4R Energy-US, Prof. Scott Moura of UC Berkeley who does research on modeling of energy systems, and Eduard Maljadi from the National Renewable Energy Laboratory (NREL)Transmission Grid Integration Group.

The project developed a simulation of the microgrid based on energy flow between components of the system and did not model the dynamics of each DER within the system. This simulation was used to predict the benefits that installing the ESS and the additional 80 kW of solar would provide to the facility. Demand data from the previous year was used as the baseline for the simulation. A 120 kW PV array already existed on the site, and data from this system was also used in the simulation. Data for the new 100 kW PV array was generated using NREL's PV Watts set for Davis, California.

As part of the project, the research team developed a control and management system to improve microgrid stability and grid interface. The control system architecture of the ESS had three levels. The first level was dedicated to functions to ensure the safety of the electrical grid and ESS. The second level was the EMS that controls the power flow in the microgrid and operates in different modes depending on operator objectives. The third level was California ISO interactive control to incorporate day-ahead demand and generation predictions, bulk pricing data, and real-time utility renewable generation ratios.

The project team equipped the smart ESS with advanced technologies that automatically diagnose, balance, and manage the second-life EV lithium-ion traction batteries. Market predictions suggested that the batteries available from EVs will outpace the demand for stationary energy storage by an order of magnitude. This will bring the cost of second-life based microgrid storage down even further and allow developers to pick and choose only the best 10-15% of retired EV batteries for their storage applications, ensuring high performance and long lifetime.

Project Results

The project met performance goals proposed, including greater than 10 percent peak shifting and maximum demand reductions. It acted as an energy buffer by storing power and shifting PV generation peak to match energy demand as needed based on generation and energy consumption, including responding to requests to reduce electricity demand during the 2020 wildfires when energy use excessively strained the grid and caused widespread blackouts.

Benefits of this microgrid include energy savings with up to 39 percent peak energy use reduction measured and can save $12,000 per year on electricity bills and reduce the carbon footprint of the microgrid by 14,000 kilograms (kg) of carbon dioxide per year. Additional improvements could be realized with further controller optimizations, different demand profiles, and different energy tariffs. This demonstration project will stimulate the market for second-life battery systems by showing that they perform reliably to the industry.

The project faced a few challenges, but major lessons learned from this project indicate limitations with current state of the market and readiness for expanding the use of ESSs. First, there are insufficient inverters available for battery systems of this size and the costs of those inverters are too high. Acquiring an inverter took the project team more than a year due to long manufacturing lead times. Because second-life batteries reduce the cost of the battery cells in the storage system by at least half, the cost of the power conversion becomes a larger fraction of the total system cost and can significantly increase the cost of energy storage. Second, due to some recent high-profile battery fires, fire departments are increasingly strict about installing battery systems. To install the battery at UC Davis, the project team spent a full year negotiating and training the local fire department on the design of the ESS. This process resulted in few meaningful design changes while posing a major challenge to project implementation.

Technology/Knowledge Transfer/Market Adoption (Advancing the Research to Market)

Principal Investigator Professor Park's laboratory has posted information about the project on the lab's website at https://research.engineering.ucdavis.edu/greentech/bwf-microgrid/. In addition, a recently published scientific paper based on data collected from this microgrid can be found in open access form at: https://www.sciencedirect.com/science/article/pii/S2352152X21005594 The laboratory also placed flyers around the UC Davis campus advertising this project, which was successful in bringing more than 20 students to work on the project in the lab. This gave the students valuable experience on an actual project to supplement their classroom education. In addition, UC Davis has made the microgrid and battery system part of their tour for groups visiting the various energy efficiency related research organizations at UC Davis.

Based on project experience, the UC Davis research team started a company called RePurpose Energy to commercialize and further develop the technology. RePurpose Energy was awarded EPIC funding under GFO-19-310 for a follow-on project that aims to validate the ability of a second-life battery system, paired with solar PV, to provide building resiliency and load shifting services for a small/medium-sized commercial building.

Benefits to California

The major advantage to installing second-life battery energy storage in a microgrid is cost reduction. Despite current cost reduction trends, lithium-ion batteries are still expensive, so utilizing retired batteries could significantly reduce the cost of ESSs. Additionally, as EVs become more popular, the number of used EV batteries available will increase significantly by up to 200 gigawatt-hours (GWh) by 2030[1].

Overall Microgrid Benefits include:

The system demonstrated up to 81 percent peak energy use reduction and an average of 39 percent energy use reduction, which saved an estimated $12,000 per year on electricity bills and was also calculated to reduce the carbon footprint of the microgrid by 14,000 kg of carbon

[1] Engel, H., Hertzke, P. *Second-life EV batteries: The newest value poolin energy storage*. McJinsey & Company (2019).

dioxide per year. Additional improvements could be realized with further controller optimizations, different demand profiles, and different energy tariffs.

Specific Benefits include:

Economic Benefits

- The annual peak time electricity use is reduced by 39%
- Annual electricity cost savings of 35%
- Maximizes the use of renewable generation
- Reduced cost of energy storage improves market penetration, making cleaner grid.

Environmental Benefits

- Carbon Dioxide (CO_2) reduction up to 70,000 kg per year (34%)
- Reduction is 91,000 kg/year if over-generation is included, 0.287kg/kWh

Winemaking Industry Potential

- Winemaking industry uses 400 GWh/year of electricity[2].
- Carbon footprint reduction of 11,000 metric tons/year.
- Peak time energy use reduction of 3,250 megawatt-hours (MWh)/year Peak time power reduction of 2 megawatts (MW)/day.

---

[2] Galitsky, C., Radspieler, A., Worrell, E., Healy, P., & Zechiel, S. (2005). *Benchmarking and self-assessment in the wine industry* (No. LBNL-59957). Ernest Orlando Lawrence Berkeley NationalLaboratory, Berkeley, CA (US).

CHAPTER 1: Introduction

In 2018, California adopted Senate Bill 100 (De León, Chapter 312, Statutes of 2018), the California 100% Clean Energy Act. Senate Bill 100 sets the goal of powering California with 100% clean, carbon-free electricity by 2045 and requires the Energy Commission, Public Utilities Commission and Air Resources Board to use programs under existing laws to achieve 100 percent clean electricity and issue a joint policy report on Senate Bill 100 by 2021 and every four years thereafter. This goal cannot be achieved using solar generation alone; overgeneration of solar during the day is already causing utilities to curtail solar generation to maintain grid stability, wasting renewable energy. In addition, the peak demand for California is in the evening when solar photovoltaic (PV) generation is minimal. Greater penetration of renewables into the grid requires energy storage to meet morning and evening peak demands before solar generation kicks in. As a result, the ESS market is booming and projected to grow exponentially. Unfortunately, ESSs are still expensive and thus are not being deployed in sufficient quantities to meet the 100 percent Renewables Portfolio Standard by 2045. Complementary changes in utility tariffs can help encourage building owners to install ESS along with PV to reduce demand charges and offset time-of-use billing; however, other incentives such as lower prices will be required for sufficient utility-scale ESSs.

One strategy to reduce the cost of energy storage is to use second-life (used) electric vehicle (EV) batteries. California has the most EVs in the United States and will likely have the largest supply of used batteries. Used batteries still maintain between 60 and 80 percent of their original capacity, meaning that they can store enough energy to act as stationary storage systems for the electrical grid. The EV market, in terms of kilowatt-hours (kWh) of energy storage, is many times larger than the stationary energy storage market and is projected to grow faster (Wood Mackenzie Power & Renewables, 2019). Stationary storage systems can therefore be built using the best 10-15 percent of retired EV batteries. Since used batteries are considered waste, they can be obtained at considerably less cost than new batteries, lowering the cost of energy storage. Another benefit is reusing EV batteries reduces the demand for new batteries for stationary storage systems, which provides additional environmental benefits such as reduced water toxicity from mining of lithium, and reduces the life cycle carbon footprint of manufacturing lithium-ion batteries by up to 70%[3,4,5,6]. However, the market is

---

[3] R. Sathre, C.D. Scown, O. Kavvada, T.P. Hendrickson
Energy and climate effects of second-life use of electric vehicle batteries in California through 2050
Journal of Power Sources, 288 (2015), pp. 82-91

[4] K. Richa, C.W. Babbitt, N.G. Nenadic, G. Gaustad
Environmental trade-offs across cascading lithium-ion battery life cycles
The International Journal of Life Cycle Assessment, 22 (1) (2017), pp. 66-81

[5] J.F. Peters, M. Baumann, B. Zimmermann, J. Braun, M. Weil
The environmental impact of Li-Ion batteries and the role of key parameters – A review
Renewable and Sustainable Energy Reviews, 67 (2017), pp. 491-506

[6] Amnesty International
This is what We Die For": Human Rights Abuses in the Democratic Republic of the Congo Power the Global Trade in Cobalt
Amnesty International (2016)

currently skeptical about second-life ESSs since few demonstration projects exist. Developing such a system with ratepayer support, as was done in this project, can demonstrate sufficient performance of second-life EV batteries for stationary energy storage. This project buillt a renewable energy microgrid using a second-life EV battery ESS.

The Robert Mondavi Institute (RMI) of Wine and Food Science at University of California (UC) Davis is a campus research community consisting of two departments and three research centers. There are 250 graduate and undergrad students and 42 faculty working on developing vines resistant to drought and disease, analyzing the complex chemistries in wine that give each their unique sensory qualities, reducing the environmental footprint of winemaking through green chemistries and reduction in energy and water, and microbial food safety. Before this project began, the RMI had 120 kW of PV panels and an 800-kW diesel generator. The project added 80 kW of PV panels and 280 kWh of ESS that used second-life lithium-ion batteries. The additional PV is a new highly efficient module provided by Solexel. The RMI building group includes a Leadership in Energy and Environmental Design (LEED) Platinum Winery/Brewery/Food Science Building and the net zero energy certified Jess Jackson Sustainable Winery Building. Annual combined electricity consumption of the two buildings is around 726 megawatt-hours (MWh), consisting of mostly laboratory and heating, ventilation, and air conditioning loads. Due to the large number of laboratories in the Jackson Sustainable Winery Building, it has an energy usage/area 50 percent higher than the average building at UC Davis (UC Davis Facilities Management Energy Conservation Office, 2020).

While the food processing industry is generally a large consumer of electricity in California, the wine industry is an especially excellent target for energy efficiency improvements due to its high refrigeration loads and large processing equipment. According to the United States Census Bureau, the U.S. had 1,956 wineries in 2007 with 971 of the wineries in California that produce about 85 percent of U.S. wine. By 2018 the U.S. wine industry had experienced huge growth, with between 8,000 and 10,000 wineries, 3,900 of which were in California and producing 61 percent to 81 percent of U.S. wine (Conway, 2019; Wines & Vines, 2014; Discover California Wines, 2018). According to a Lawrence Berkeley National Laboratory (LBNL) study, the California winemaking industry consumes more than 400 gigawatt-hours (GWh) of electricity annually, making it the second largest electricity-consuming food industry in California, after fruit and vegetable processing. Much of the electricity used in winemaking goes toward refrigeration for cooling and cold storage. The rest is mainly used for compressed air, hot water, or electricity for pumping and bottling line equipment. The high energy use of wineries is characteristic of the food processing industry in general. Food processing is the third largest energy user in California, which is the top agricultural state in the nation. According to a 2008 report by the California Energy Commission,[7] California's food processing industry generates more than $50 billion in gross annual revenues.

By reducing the cost of commercialized second-life ESSs, the adoption of battery systems and microgrids would likely accelerate, increasing California's electric reliability and reducing greenhouse gas (GHG) emissions. Additional energy storage would allow for a greater fraction of renewable energy resources on the electrical grid while reducing fears of their intermittency

[7] California Energy Commission. 2006. *California's Food Processing Industry Energy Efficiency Initiative: Adoption of Industrial Best Practices* (Publication Number CEC 400-2008-006-REV).

and non-dispatchability. By shifting peak demands, the grid can be operated more efficiently which will reduce costs and environmental impacts.

Project Goals and Objectives

To meet legislative requirements for reducing GHG emissions, California must increase the use of renewable energy while maintaining reliability of the electrical grid. Distributed energy resources (DER) are an effective means for attaining this goal. These systems help provide energy security for communities by providing locally generated power while improving grid stability through peak load reduction and improved renewable-to-grid integration.

The overarching goal of this project was to develop an economical second-life battery energy management system (EMS) to effectively measure and control state of charge (SoC - the level of charge in an electric battery relative to its capacity) and state of health (SoH - the general condition of a battery and its ability to deliver the specified performance compared with a fresh battery). This project developed a renewable energy microgrid using second-life EV batteries to demonstrate that second-life batteries perform well enough to be used as stationary systems

s, thereby reducing the environmental impact of adding energy storage to the utility grid. The project team developed and demonstrated a smart electrical ESS using retired EV batteries. The ESS provided a cost-effective and efficient energy storage solution for a community-scale grid with multiple renewable generators. The ESS acts as an energy buffer, storing power and shifting energy from peak solar PV generation to peak grid energy consumption.

This project demonstrated that the technology required to build a reliable and green electrical grid currently exists and can be deployed at a local level. Implementing community-scale microgrids can reduce the effects of public safety power shutoffs due to insufficient grid infrastructure. Inexpensive energy storage built using second-life EV batteries, expected soon to be an abundant resource, can make communities self-sustaining even when the power grid is shut off. This project will provide ratepayer benefits of greater electricity reliability and lower costs by improving grid reliability, reducing peak demand, and producing and storing energy that can be sold in the California ISO electricity market. With the support of the ESS and proper energy management control, the microgrid can be run at maximum renewable generation of up to 100 percent. The ESS and EMS not only maximize the use of renewable generation but also can support the sale of excessive production (or even some portion of PV generation) through the demand response (DR) or California ISO market.

The results of this project provide performance data of second-life batteries in a microgrid environment, and are of special interest to industry groups, government policy makers, and academics studying energy systems.

Project Goals

The goals of the project were to:

- Demonstrate 100 kW of high-performance, precommercial solar PV generation.
- Develop and demonstrate 250 kWh of second-life lithium-ion battery energy storage.
- Develop and demonstrate an advanced EMS capable of peak reduction, load shifting, and DR.
- Commission, validate, and test the microgrid system.
- Operate the power generation and management system for at least 12 months, collect performance data, and optimize the system to shift energy most effectively from peak renewable generation to peak energy consumption and to tune the EMS controller to mitigate grid instabilities.
- Calculate reductions in electrical demand and emissions. Demonstrate that the energy generation and management systems reduce the community's average daily power demand and daily peak energy/power demand by more than 10 percent (with a stretch goal of 60 percent).
- Demonstrate that system operation will significantly reduce the community's average electricity cost.
- Demonstrate that the system can perform autonomous frequency and voltage control to mitigate grid instability caused by the operations (charge/discharge) of electrical energy storage.
- Document and publish results and lessons learned.

Project Objectives

The objectives of this project were to:

- Demonstrate that the system operation would result in more than 10 percent reduction (stretch goal 60 percent reduction) in the difference between the community's average daily peak power demand and the average daily power demand placed on the grid by the community.
- Demonstrate that the system operation would result in more than 10 percent decrease (stretch goal 60 percent decrease) in the daily average energy demand during peak times, as defined by the utility tariff, placed on the grid by the community.
- Demonstrate that the system would reduce the community's annual average electricity cost by more than 10 percent.
- Demonstrate that the autonomous frequency and voltage control would reduce the System Average Interruption Duration Index (SAIDI) [8] by more than 50 percent.
- Demonstrate that the system could be profitable by selling ancillary services to the California ISO fast regulation market and participating in DR. The project team

[8] The electric distribution System Average Interruption Duration Index (SAIDI) is a description of the length of time all customers would have been out of power if the total number of hours out of service in a year's time were to be shared, and it is typically measured in minutes.

expected that DR would maximize the economic benefit of the system, but could also sacrifice peak reduction/load shifting, which was the main goal of the project.

Project Team

- Professor Jae Wan Park served as the principal investigator for this project. Park was responsible for microgrid controller hardware design, installation, testing and demonstration. Park was also the technical coordinator for project teams including UC Davis centers and contractors.
- Jill Brigham served as the project manager, with her responsibilities including coordination between the project team and the university as well as third party partners. In addition, she oversaw project budgeting.
- Dr. Masoud Rahman, Professor Park's lab manager, worked on system engineering and controller design.
- Joseph Lacap, a Ph.D. candidate, was responsible for simulation of the microgrid, development of day-ahead renewable energy and load forecast, reviewing the microgrid communication protocol and standards, energy management and flow analysis, and ESS design.
- OSIsoft provided the data management and visualization system for the project as match funding.
- Auxin Solar supplied the commercial high efficiency solar panels for the microgrid.
- Rhombus Energy System supplied the bidirectional multiport battery inverter for the project.
- The UC Davis Fire Department participated in safety reviews and training of the design of the microgrid.

CHAPTER 2: Project Approach

Project Overview

The system consisted of a utility-connected microgrid on the UC Davis campus. The renewable power for the microgrid was generated from 200 kW of PV panels across two arrays, of which 80 kW were added under this project and 120 kW were installed prior. An ESS with a nominal capacity of 280 kWh was installed to facilitate peak shifting, peak shaving, and make use of solar over-generation. To implement this system, the project team developed power conditioning, data collection, data storage, and control systems to optimize the use of PV generation and energy storage while maintaining the microgrid's stability.

Figure 1 shows a schematic of the system. All loads and DERs were connected to a three-phase 480-Volt (V) alternating current (AC) bus. Power, data, and control flows are shown with red representing power (AC, direct current [DC], and voltage is labeled), blue representing data, and green representing control. All system data is gathered, stored, and analyzed in the plant information (PI) server, cornerstone of the EMS.

Figure 1: Microgrid Architecture

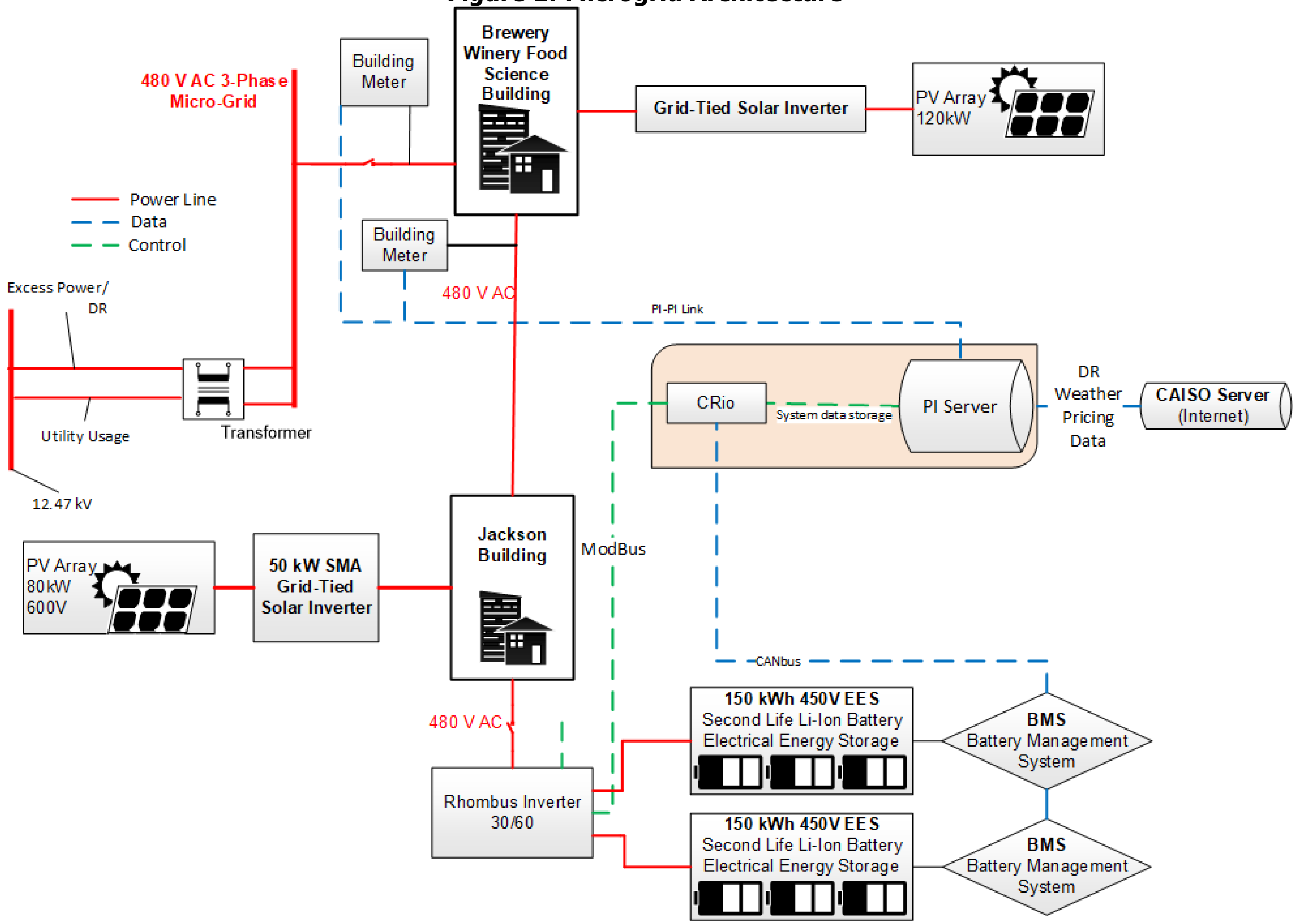

Microgrid system architecture showing power, data, and control connections.

Source: UC Davis

The ESS system consists of two battery systems (strings) connected to the microgrid through a 60-kW Rhombus Energy Solutions inverter. A string is a set of cells, modules, or assemblies connected in series. The nominal capacity of each battery string is 200 kWh (for a total of 400 kWh); however, the second-life cells have a SoH of 75 percent, meaning the actual capacity is 150 kWh. The research team limited the batteries' SoC to the 20 percent to 80 percent range to increase the service life of the batteries. This reduced the available capacity of each system to 90 kWh, adding to a total of 180 kWh between the two systems. To build the battery pack from second-life battery cells, the project team extensively tested every battery module. The researchers developed optimization algorithms to match battery modules together based on their measured internal resistance and SoH in such a way that the service life of the end system would be maximized.

The project team wrote the microgrid controller in Labview to be compatible with the National Instruments compactRIO 9037 that was selected as the microgrid's central control hardware. The team selected this dedicated controller for its modular input/output (I/O) architecture, which enabled the control and measurement of external data sources not possible with a standard computer. Each battery management system (BMS)is connected to the controller by CANbus, and the controller communications with the inverter over Modbus. The controller acts as the microgrid's EMS and dictates when the batteries should be charged and discharged. This system also ensures safe operation of the battery. Custom control software was written such that new battery control modes could be tested to optimize the microgrid for various scenarios, including carbon footprint reduction, demand charge management, peak time energy use reduction, and dynamic control based on overall demand and price in the California ISO region.

The research team developed a software simulation of the microgrid in Matlab. This simulated microgrid was used to predict the benefits of installing the ESS and additional solar at the facility. The simulation was based on energy flow between components of the system but did not model the dynamics of each DER within the system. Historical data was used as the baseline for the simulation, including demand data from the previous year and data from the pre-existing 120-kW PV array onsite. Data for the new 80-kW PV array was generated using National Renewable Energy Laboratory (NREL) PV Watts set for Davis, California (National Renewable Energy Laboratory, 2017). The results of this simulation suggested that the microgrid would reduce the carbon footprint of the associated buildings by 10 percent, or 14,000 kilograms (kg) carbon dioxide (CO_2) per year. Peak demand was predicted to be reduced by 40 percent, and the average energy use during peak hours was predicted to be reduced by 33 percent. As a result, the simulation predicted bill savings of $12,000 per year, or 14 percent.

Second-Life Energy Storage System

This section reviews the ESS system design for the project and describes each subsystem, interface, control, and concept of operation. The main goal of this system was to store sufficient electrical energy to reduce the peak power demand of the microgrid by at least 10 percent while achieving a charge/discharge efficiency of at least 80 percent. The secondary objective is to utilize second-life EV lithium-ion batteries for increased system sustainability. The ESS system is connected to the RMI microgrid composed of the Jackson Sustainable Winery Building and the Brewery Winery and Food Science Building.

Second-Life Electrical Energy Storage Design Overview

Figure 2: Photo of Microgrid

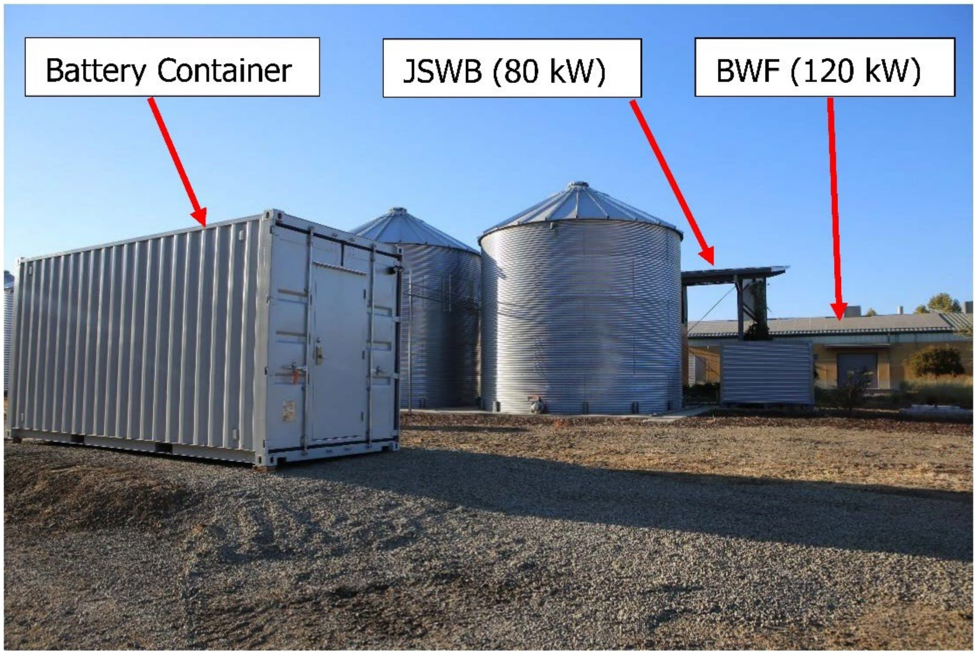

Photo of the microgrid showing the battery system in a 20ft shipping container, the Jackson Sustainable Winery Building , and the Brewery Winery and Food Science Building.

Source: UC Davis

Figure 3: Inside the Battery Container

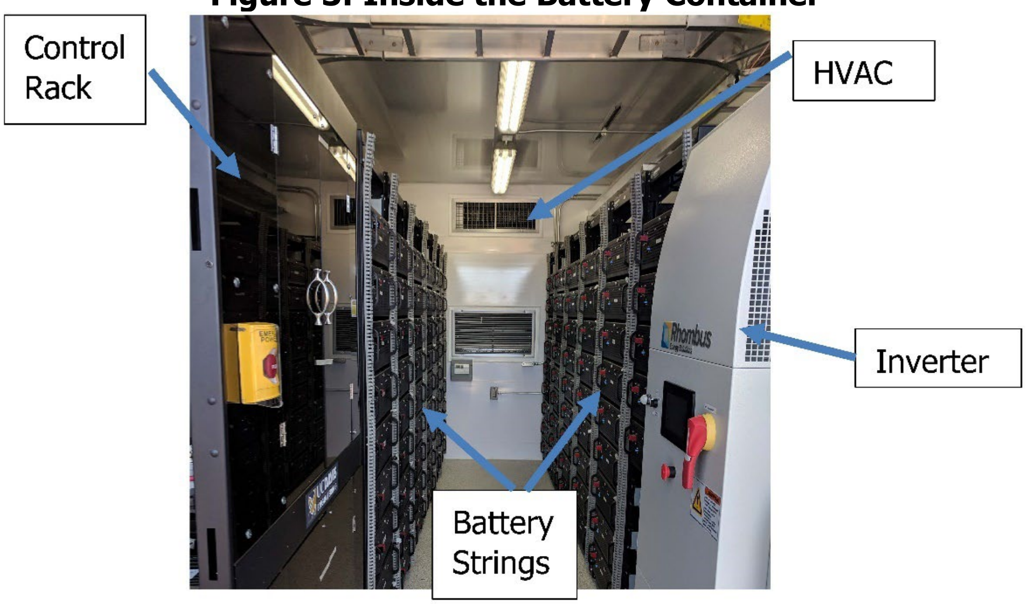

Inside the ESS container. Left: Control and high voltage switching rack. Right: Inverter. Back: Battery racks

Source: UC Davis

Each battery system was built modularly. The used battery modules from 18 Nissan LEAFs were packaged together and connected in parallel to form an assembly. These assemblies were connected in series to form a bank. The voltage of the system was 450V. Charging and discharging was controlled by the EMS, subjected to the safety limitations imposed by the BMS.

Figure 4 provides an overview of the battery's construction and how the battery banks were connected in series in the shipping container. The BMS collects data from all parts of the battery and uses this information to ensure the battery is operating safely. Figure 5 shows a more detailed diagram of the construction of a battery bank. It shows each assembly in the rack including the connections to adjacent assemblies and to the BMS.

Figure 4: Wiring Overview of Energy Storage System

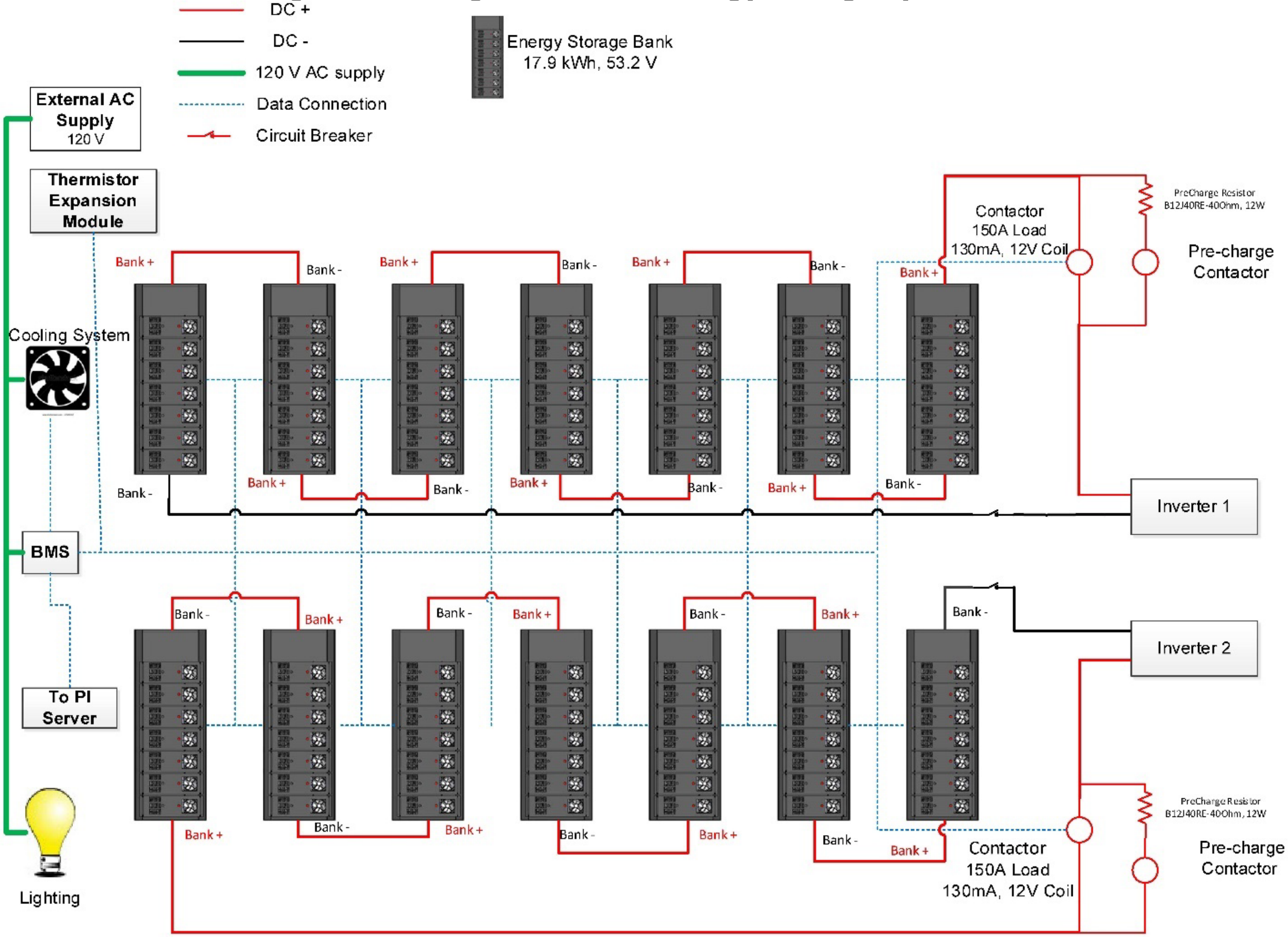

Diagram of ESS System showing banks connected in series along with BMS gathering data from the banks and sending data to PI server.

Source: UC Davis

Figure 5: Battery Bank Wiring Connections

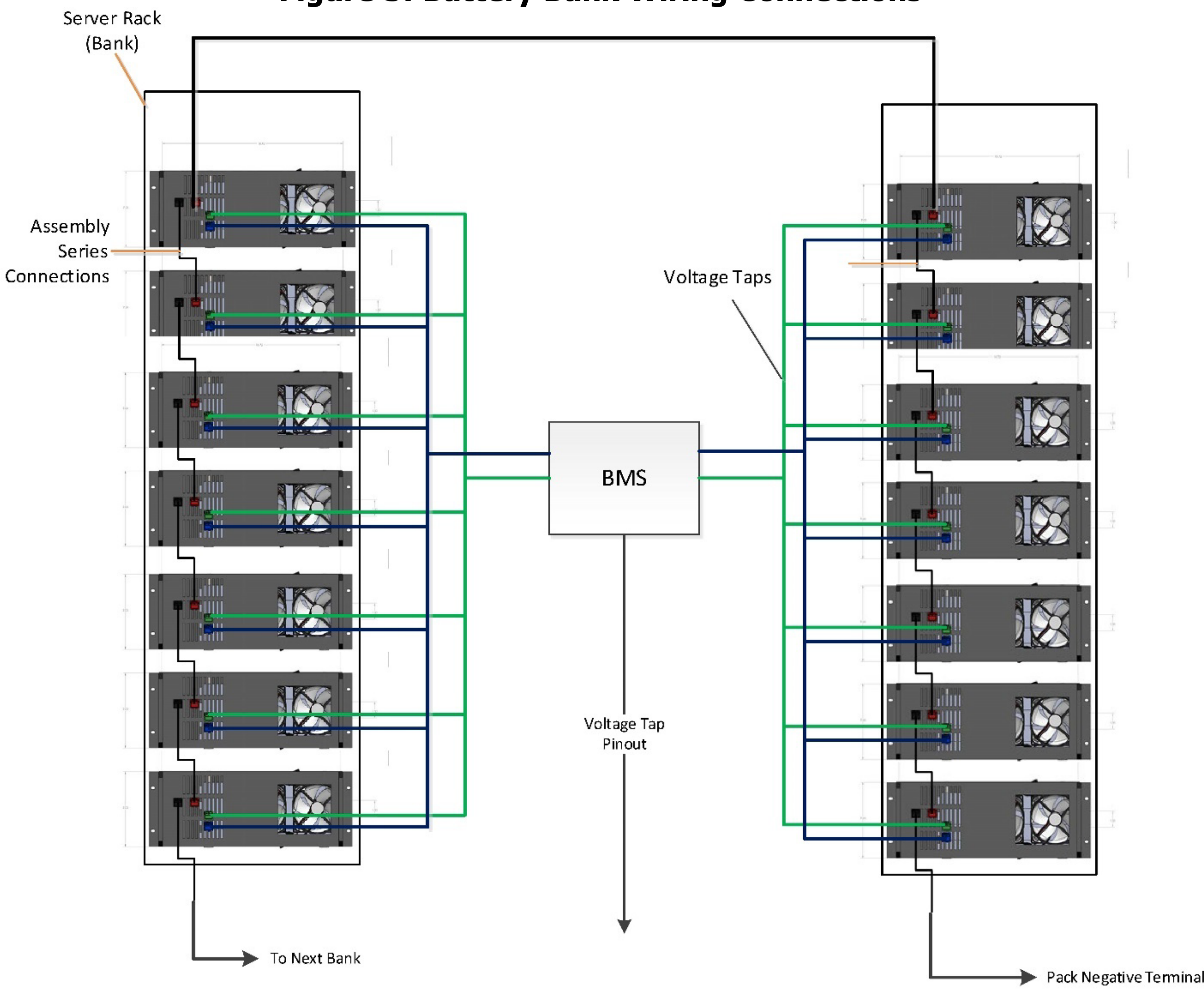

Detailed diagram of ESS connection to BMS voltage taps and assembly series connections.

Source: UC Davis

The ESS is composed of several components in three categories: energy storage, power conditioning, and management (safety and control). Four levels of energy storage were defined for the system, corresponding to the level of modularity.

1. The first, lowest, level is the battery module. (Figure 6). This is the basic unit of the ESS, as supplied by Nissan.
2. The assembly is the second level. It is made up of 8 modules connected in parallel and housed in a server case. (Figure 7).
3. The bank is the third level. Nine battery assemblies were connected in series in a server rack. (Figure 5).
4. The string is the final level, consisting of 6 banks connected in series. (Figure 3).

Figure 6: Nissan LEAF Battery Modules

Nissan LEAF battery modules. Left: bottom of module. Right: Top of module.

Source: UC Davis

Figure 7: Battery Assembly

An assembly of Nissan LEAF Modules. It contains 8 modules connected in parallel. The large connectors on the front are the assembly terminals, the small blue ports are the voltage taps for the BMS.

Source: UC Davis

The power conditioning for each battery pack is performed by the Rhombus Energy Systems 30/60 Inverter enclosed inside the battery container (Figure 3). This 60kW bi-directional inverter both charges and discharges the batteries, eliminating the need for a separate charger. It also has two DC ports that were electrically isolated from each other. This means that each battery string is a separate battery pack such that one can continue running while maintenance is being performed on the other. Each battery pack has its own inverter, but the AC side of the inverters were internally paralleled and act as one. The inverter output passes the power through an integrated transformer for isolation before the power is supplied to the microgrid.

The BMS is the primary method of battery control. It measures the state of the battery pack and individual battery assemblies and determines the ability of the pack to supply and store energy. When the EMS requests charge or discharge, the BMS must "approve" the request to ensure operational safety. The BMS is responsible for the safe operation of the ESS, ensuring the temperature, current and voltage limits were not exceeded. It can disable all charging and discharging for the battery pack and control the ESS thermal management system.

The EMS controls when and how much to charge or discharge the ESS. It controls the inverter to maximize grid stability, power quality, and peak shaving using energy stored in the ESS. The EMS is outside the system boundary of the ESS, but it must interface with the BMS in such a way as to obey limits imposed by the BMS. The interface between the BMS and the EMS uses the highly noise resistant CANbus communication protocol.

Energy Management System

This section reviews the controller architecture and the code development process. The controller hardware requirements have been reviewed in detail in a separate document. The controller is required to do the following tasks:

1. Collect data from BMS, inverter, building load, weather forecast, and California ISO.
2. Run the EMS based on the selected algorithms such as peak shaving, peak shifting, maximum revenue, power quality, power reliability/backup, and California ISO DR market.
3. Send control commands to the inverter and the switches/breakers.
4. Export the data for visualization and storage to the OSIsoft PI server.

Figure 8 shows the controller communications and input/output (I/O) architectures.

Figure 8: Controller Input and Output Diagram

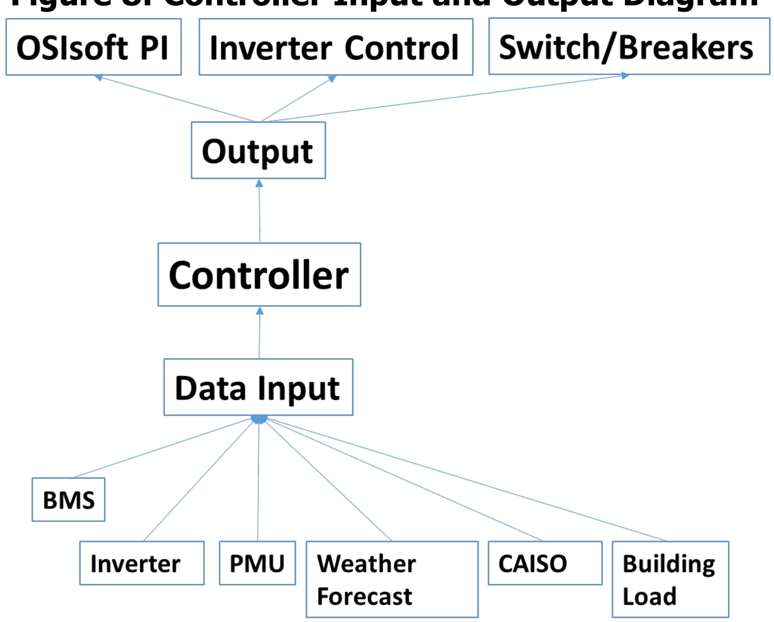

Controller input/output Communications with other devices and databases.

Source: UC Davis

The controller hardware was purchased from National Instrument and has the following components:

1. NI 9862 CAN interface module for communication with the BMS.
2. NI 9475 Digital output for control of the contactors, battery fans.
3. NI 9421 Digital input module for connecting to the ground fault detection interruption.
4. NI 9037 CompactRIO Controller and Processor.
5. NI 9472 Digital output module.

Figure 9: Controller Hardware

Integrated Controller and Chassis

Part Number	Description	Quantity
784549-01	cRIO-9037, 8-Slot WiFi CompactRIO Controller	1
	Standard Repair Coverage	1

Modules

Part Number	Description	Quantity
780132-01	NI 9475 8-Ch 60 V, 1 us, High-Speed Sourcing Digital Output	1
	Standard Repair Coverage	1
781922-01	NI 9924 Front-mount terminal block for 25-pin D-Sub Modules	1
781639-01	NI 9862, C Series, CAN Interface, High-Speed/FD, 1 Port	3
	Standard Repair Coverage	3
780041-01	NI CAN Breakout Box 7-Port for CAN, DeviceNet, and CANOpen	3
782578-02	NI CAN No Termination Cable w/Power Terminals, HS/FD/LS, 2m	3

National Instruments parts used in the system controller.

Source: National Instruments

The controller has a three-level hierarchical structure. The components of the controller are as follows:

1. Data input from BMS and inverter.
2. Data import from OSIsoft PI server such as building load, weather data, and California ISO data.
3. Controller level 1: this controller is responsible for safe and reliable operation of battery packs and inverter.
4. Controller level 2: this controller is responsible for operation optimization such as peak shaving, peak shifting, and maximum revenue operation.
5. Controller level 3: this controller is responsible for California ISO DR market participation.
6. Data export to OSIsoft PI server for data archive, data visualization, and performance analysis.

Figure 10: Controller Design Overview

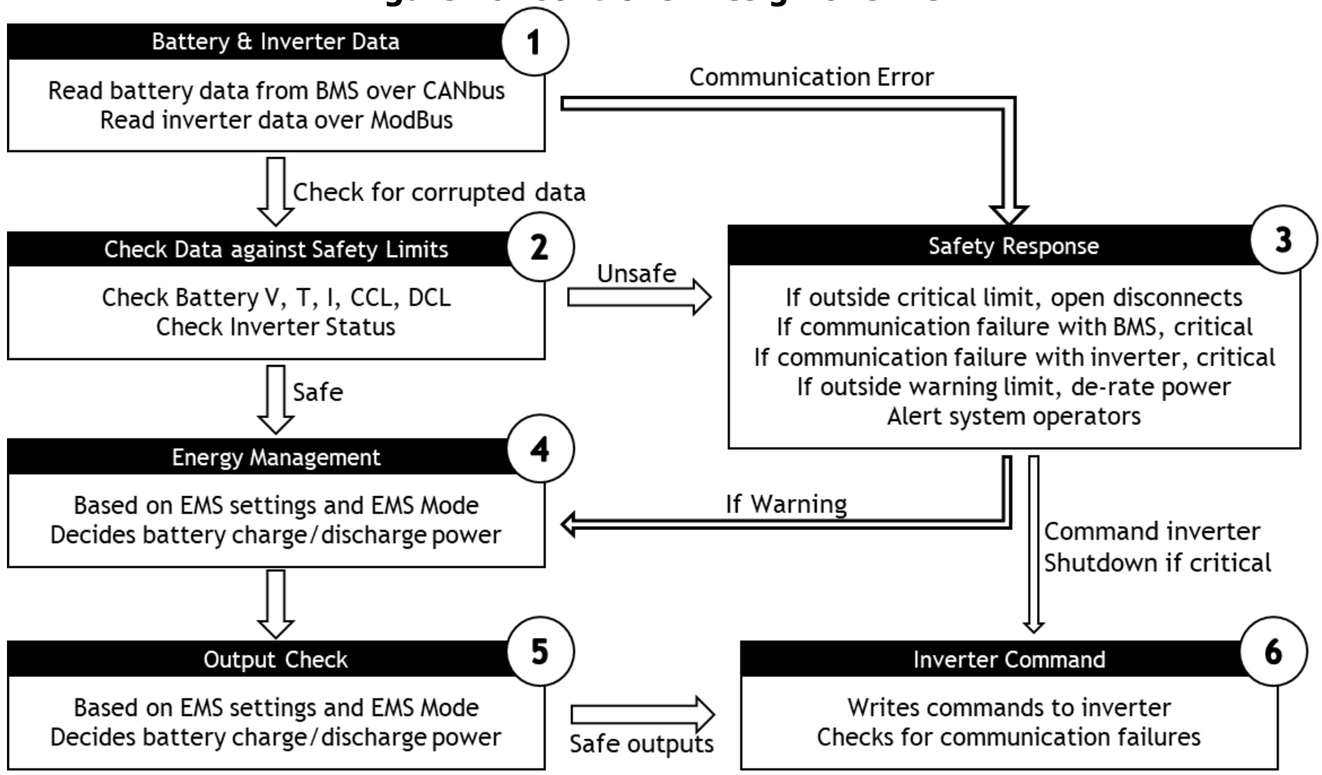

Controller architecture diagram highlighting safety features.

Source: UC Davis

Controller Safety

The controller was developed with battery safety as the top priority. The voltage, current, and current limits were constantly monitored, and every decision the controller made was checked against the limits. Figure 10 shows the flow of decisions the controller makes and how the safety checks affect them. In step 1 of the controller, data is read from the inverter and BMS. The functions that read the data check for communication errors and corrupted data. If an error persists for more than one second, step 3 is triggered which results in a critical error, opening battery disconnect switches and shutting off the inverter.

If communications are working, the data is passed to step 2 which checks the data against set limits and dynamic limits such as calculated charge and discharge current limits which are a function of battery state. If any parameter is outside the safe range, data is again sent to step 3. If the parameter is outside the critical safety range, the same response as a communication error is triggered. If the parameter is above the warning limit but below the critical limit, the battery current limits are reduced to derate system power.

In step 4, the EMS decides what the battery should do. Multiple possible energy management modes are included in the controller (described below). The energy management function can request any power within the operational limits of the inverter, but the battery may not always be able to meet this request. Therefore, after the energy management function runs, the controller's final inverter commands are once against checked in step 5, which performs the same functions as step 2 in addition to coercing the output to be within the safe operating range.

Additional safety features were built into the hardware of the system, including the BMS, inverter, and manual controls. The BMS is connected to the battery disconnect switches and can open them without “asking” the controller. Likewise, the controller can open the switches without asking the BMS. Additionally, the disconnects were connected to the system emergency power off (EPO) switch so that the battery will be immediately disconnected in the event of an emergency. Disconnects were also placed in the middle of each battery string so that the controller and the EPO can break the battery circuit, cutting the battery voltage in half. If the controller loses communication with the inverter, the inverter will turn itself off. If the battery disconnects were opened, the inverter detects that the battery is no longer connected and shuts down. When the controller detects any error, it sends both SMS and email messages to personnel listed as system operators.

Controller Energy Management

The controller code was developed modularly so that it can operate in various energy management modes. The code was simple to develop and will allow additional modes in the future. This lets the microgrid system be used as a real-life test bed for piloting new battery control algorithms. To date, the developed modes are:

- Manual mode
    - Manual mode is used for debugging, demonstration, and system startup. It allows all functions of the controller to be set manually. However, if unsafe commands are sent to the inverter, the BMS can disconnect the battery from the inverter, maintaining the system’s safety.
- Time-based peak shifting
    - This is the simplest energy management mode. It requires no feedback from the microgrid. It discharges the battery at constant power during a set time interval and charges the battery with a constant power, constant voltage (CPCV) charging methodology during a set time interval. While CPCV results in higher current during the low-voltage section of charging, the battery current is still low since the maximum current the inverter can charge or discharge the battery with is 111A, and the battery is 360 Amp-hours. In practice, the current does not exceed 60A.
- Load-leveling
    - This mode keeps the net demand of the microgrid on the utility grid constant. The target load is set manually. The charge and discharge power of the battery is adjusted using feedback from the utility meter to keep the demand as level as possible.
- Maximum peak-shaving
    - This mode sets a “power ceiling” and a “power floor” for the next 24 hours based on the predicted net load/solar generation. If the load is above the ceiling, the ESS is discharged. If the load is below the floor, the ESS is charged. The ceiling and floor are calculated based on a prediction of the net demand without the ESS. The ceiling is lowered until the predicted battery discharge energy is equal to the allocated discharge energy. This allows for reserve capacity in the battery to compensate for prediction error. Similarly, the power floor is raised until the predicted charge energy is equal to the predicted discharge energy. This

prevents the battery from being depleted for the day after the prediction. The effect of this mode is to maintain the microgrid net demand within a certain window which helps improve grid stability.

System Simulation

In the Matlab simulation of the microgrid, first the site demand and PV data were loaded to generate the net demand before the microgrid installation to establish a base case for the simulation. Next, the additional 80 kW of PV was added to the model to generate a new net load. Then the simulation performed energy management functions, which consisted of peak shaving, peak shifting, and load leveling. The peak shaving function was able to be set manually or automatically to calculate the maximum allowed demand. The results below were generated using manually set definitions of peak power for each month as in Table 1. If the microgrid demand is above the values in Table 1, the ESS is dispatched to keep the demand at or below this value.

Table 1: Simulation Peak Power

Jan	Feb	Mar	Apr	May	Jun	Jul	Aug	Sep	Oct	Nov	Dec
85	75	70	70	67	75	55	75	70	75	75	79

Set definitions of peak power (P_{peak_t}) for each month. (kW)

Source: UC Davis

When set to automatic calculation of peak power, the simulation used historical data for each month to calculate the average deviation from the average demand.

Peak shifting was based on the (configurable) time of day, such that it would attempt to charge and discharge the battery at set times and at either a set or calculated power. This was typically used for time of use electricity tariffs. The load leveling section of the EMS is like peak shaving, but also accounts for demand that is lower than a specified value, in this case zero kW. Thus, if the building net demand due to PV over-generation was less than 0 (sending power back to the grid), then the battery would charge to prevent power form being exported to the utility grid.

Once the energy management functions were run, the simulation compared the requested battery power by the model to the battery's current SoC and max power. The battery is set to meet all requests until it is fully discharged or fully charged. If the power demand is higher than the maximum battery power, the battery partially meets the requested power. The simulation then generates a battery power output that is added to the load data to generate the final net demand.

The electricity cost savings used in the model are based on the PG&E E19-TOU electricity tariff (Pacific Gas and Electric Company, n.d.). The carbon footprint was calculated based on 2014 data for California's electricity mix based on the California Energy Commission's stipulation in the grant documents. The data was from the Energy Information Administration's *California Electricity Profile 2014* (U.S. Energy Information Administration, 2014). This data gives the carbon intensity of California's grid as 633 lbsCO_2/kWh (0.287kgCO_2/kWh). The most recent data currently available on the EIA's website is for 2017, with a more up-to-date figure of 0.215kgCO_2/kWh.

Figure 11: Peak-Time Energy Use Reduction

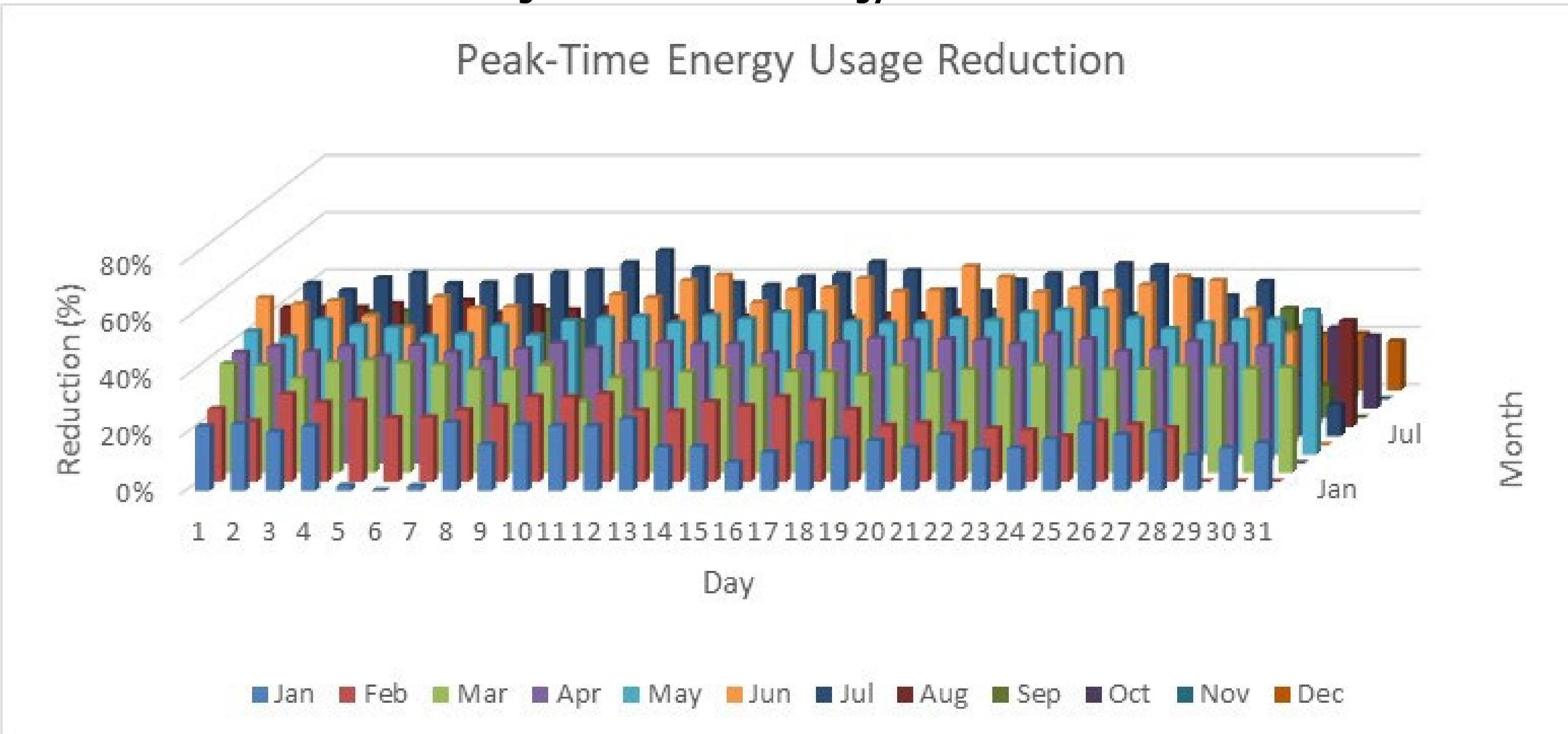

Simulated daily peak-time energy usage demand reduction.

Source: UC Davis

Technical Problems and Challenges

The first problem identified was related to constructing the second-life battery system. To build a practical ESS from second-life battery cells, each cell had to be tested and characterized. This meant battery testing took much longer than was practical. To address this, the research team purchased an additional battery test station to accelerate battery testing. Since the SoH of the cells were non-uniform, they could not be randomly reassembled into assemblies. When battery cells have mismatching internal resistance or capacity, the current distribution between the cells is uneven, resulting in some cells aging faster than others, which lowers the system's lifetime (Gogoana, Pinson, Bazant, & Sarma, 2014). Maximizing the system's lifetime required extensive testing of the battery cells. This testing was performed over a period of 11 months, during which the internal resistance and capacity of all 1081 Nissan LEAF modules was characterized. Figure 14 shows the results from the capacity testing. While the results in Figure 12 is consistent with the general consensus from literature that second-life batteries have 70-80 percent of their capacity remaining (Debnath, Ahmad, & Habibi, 2014; Saxena, Le Floch, MacDonald, & Moura, 2015), the research team suspects that the cells received were prescreened to be the higher end of the SoH spectrum. This concern was raised due to conversations with industrial battery suppliers who have a large number of second-life EV batteries in storage, and it is also supported by some literature (Saxena, MacDonald, & Moura, Charging ahead on the transition to electric vehicles with standard 120 V wall outlets, 2015).

Figure 12: State of Health Distribution of Nissan LEAF Modules

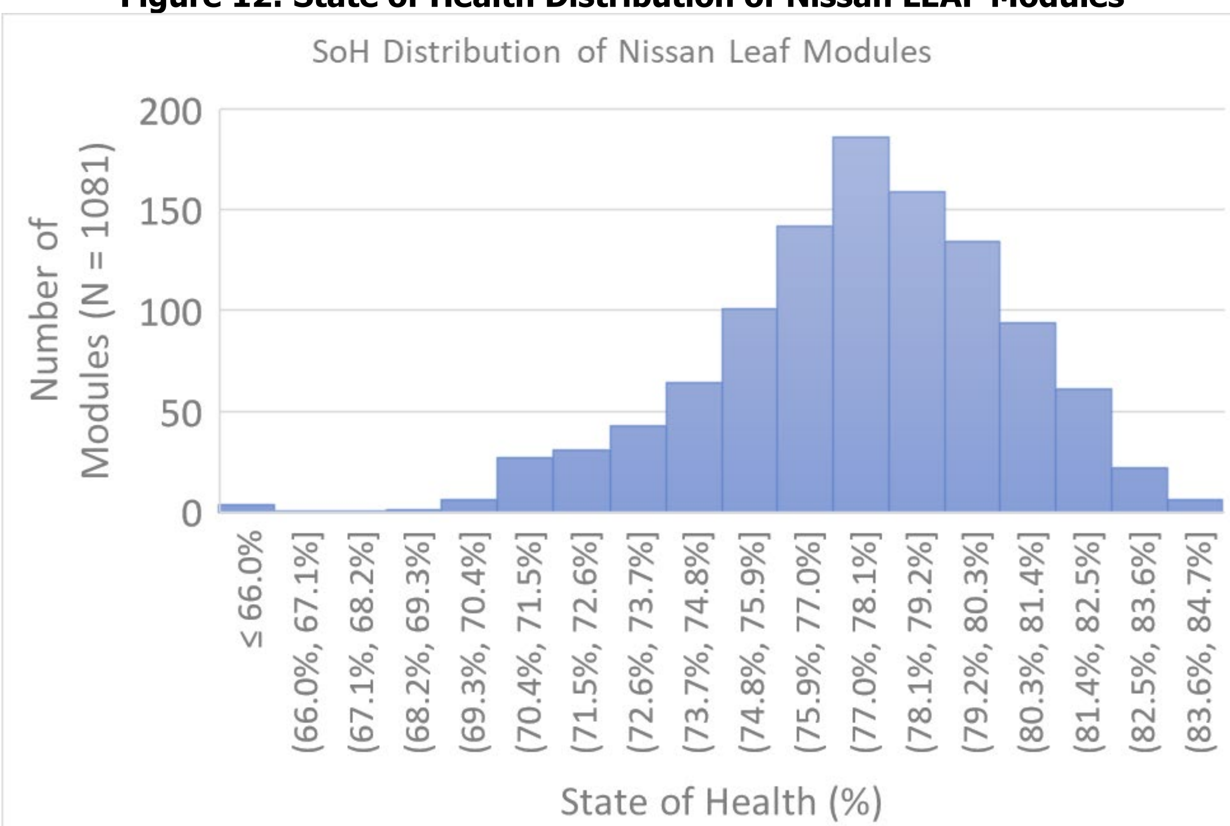

The Second-Life Modules State of Health Distribution.

Source: UC Davis

The second problem was related to securing the battery inverter. At the time of purchasing an inverter, there were only five companies with products that fit the required technical specifications of the project. Of those five, only three were able to meet the requirements for spending funding in California, one of which was prohibitively more expensive than the others. After having chosen an inverter, signing a purchase agreement, and waiting the nine-month lead time, the manufacturer informed the researchers that they had stopped making inverters for this market segment. At this point, the project team turned to the final remaining company and had to wait for another one-year lead time. The delay in procuring an inverter caused delays with integration engineering between the EMS and the inverter. A problem with the inverter's internal communication board's power supply was discovered, and it took several additional months to resolve this. Once communication was established between the controller and the inverter, testing of charge/discharge performance of the batteries using the inverter revealed additional communications issues. The inverter generated too much interference for its own communications circuits, which resulted in it losing contact with the controller. This malfunction took the manufacturer months to resolve, and this lasted two months into the demonstration period. Every time communication was lost, the entire system would shut down as an intended safety feature.

Another technical challenge arose from the ripple current (AC signal superimposed on the DC side) in the battery inverter, which can be up to 50 percent of the average current draw due to the nature of converting from DC to AC. This meant that when the inverter was drawing 20 Amps (A) from the battery, the actual current draw was between 10 and 30A. The BMS was sensitive enough to detect this variability in current. For example, the BMS may have the maximum safe current set at 50A, and the inverter may be commanded to discharge at 40A, but due to the current's ripple effect, the maximum current drawn could reach 60A, above the limit imposed by the BMS. This will result in the BMS shutting down the system once it detects this over-current. Since the researchers had no control over the firmware of the BMS, the team could not tell the BMS to use the average current over a period (such as one second), which would have been the ideal way to solve this problem. Instead, the method chosen was to program the controller to give the inverter a lower current limit than what was set by the BMS. This way, the controller automatically lowers the requested current if the maximum current value is operating near the BMS current limit. Although this had the possibility of reducing the maximum power of the battery pack, since the current of the battery was designed to be more than double the nominal operating current, this did not practically affect the operation of the battery.

The battery was designed as a floating system such that no battery terminal is referenced (or connected to ground). The advantage of this approach is the battery pack fault becomes tolerant to isolation failures. If, for example, the negative terminal of the battery was referenced/connected to ground, and a ground fault were to occur at the positive terminal, then the battery pack would be short circuited through ground, posing a danger to the battery. With the floating battery approach, no current is induced by a battery terminal becoming referenced to ground, except a small capacitance (which may still carry a high voltage). Despite this design, the BMS detected a ground fault in one of the two battery strings, meaning that a wire connected to one of the battery terminals formed a connection to ground. This fault could have resulted in damage to power electronics or a potential shock hazard to personnel and indicated that a failure has occurred in the system, even if the danger is not immediate. Once detected, the string was shut down, and the maintenance switch was opened to reduce the pack voltage to make troubleshooting safer. After two days of careful diagnosis, it was determined that the faulty component was the string's discharge contactor. The contactors apparently possess a failure mode in which the high voltage/current terminals can become connected to the low-voltage control terminals. Since the control voltage was referenced to ground, the result was the positive terminal of the battery being grounded whenever the contactor was closed. Once this was determined, the control electronics were redesigned with higher quality contactors, which allowed the project team to reduce the number of contactors from four to two. This lowered the number of failure points, simplifying the battery design and reducing heat loss by approximately 100W. However, due to this redesign and the need to order new parts, the battery string remained offline for some time. Fortunately, the modular design of the battery allowed the other remaining battery string to continue operating during this time, but the benefits seen in the following section were reduced in June-September due to this string failure.

CHAPTER 3: Project Results

In general, the project has mostly met the goals and objectives laid out in the scope of work. Originally, 100 kW of precommercial PV was to be installed by Solexel, but the company's financial situation prevented it from providing the panels for this project. In addition, changes to the fire code reduced the number of panels that could be installed on the building, resulting in only 80 kW of PV being installed, but with the inverter being provided as match funding by SMA America.

The goal for energy storage was to demonstrate a 250 kWh second-life ESS along with an EMS capable of peak reduction, load shifting, and DR. The system was too small to qualify for DR programs, but the rest of the project goals were accomplished. The system was validated, including all safety systems both in the lab and at the installation site.

The microgrid achieved the following metrics for the first 2 years of operation:

- Peak-time energy use: down 29 percent
- Max peak-time demand: down 64 percent
- Electricity bill: down 35 percent*
- Carbon footprint: down 34 percent*
- Solar self-consumption: up 60 percent
- Peak-time renewable energy mix: up 28 percent

The microgrid has operated for two years – a year more than planned in the original scope of work. During this time, the EMS operated in time-based peak shifting mode to fulfill the system's primary goal of minimizing microgrid demand during peak hours. In PG&E territory, peak hours are 4 p.m. to 9 p.m. (Pacific Gas & Electric Company, 2018), and the EMS is set to discharge at 30 kW during that time. The system charges during the day when PV generation is highest. Charging power is set to 40 kW from 9:30 a.m. to 3:48 p.m. Data for the entire operational period has been recorded in the OSIsoft PI system. This data includes information from the BMS about the state of each battery assembly, solar generation, battery charge and discharge energy, building energy use, and estimates of overall renewable energy consumption.

The controller and ESS did not mitigate grid instability, again due to changes in the project team (OSIsoft decided they could no longer provide the control algorithm for grid stability) and capabilities of the inverter (which were changed due to selection of a more cost-effective inverter). Additionally, there were no opportunities to demonstrate the microgrid's reliability due to the UC Davis power grid's high stability.

* Values based on simulation results

Figure 13: Peak-Time Power and Energy Reduction (Battery Only)

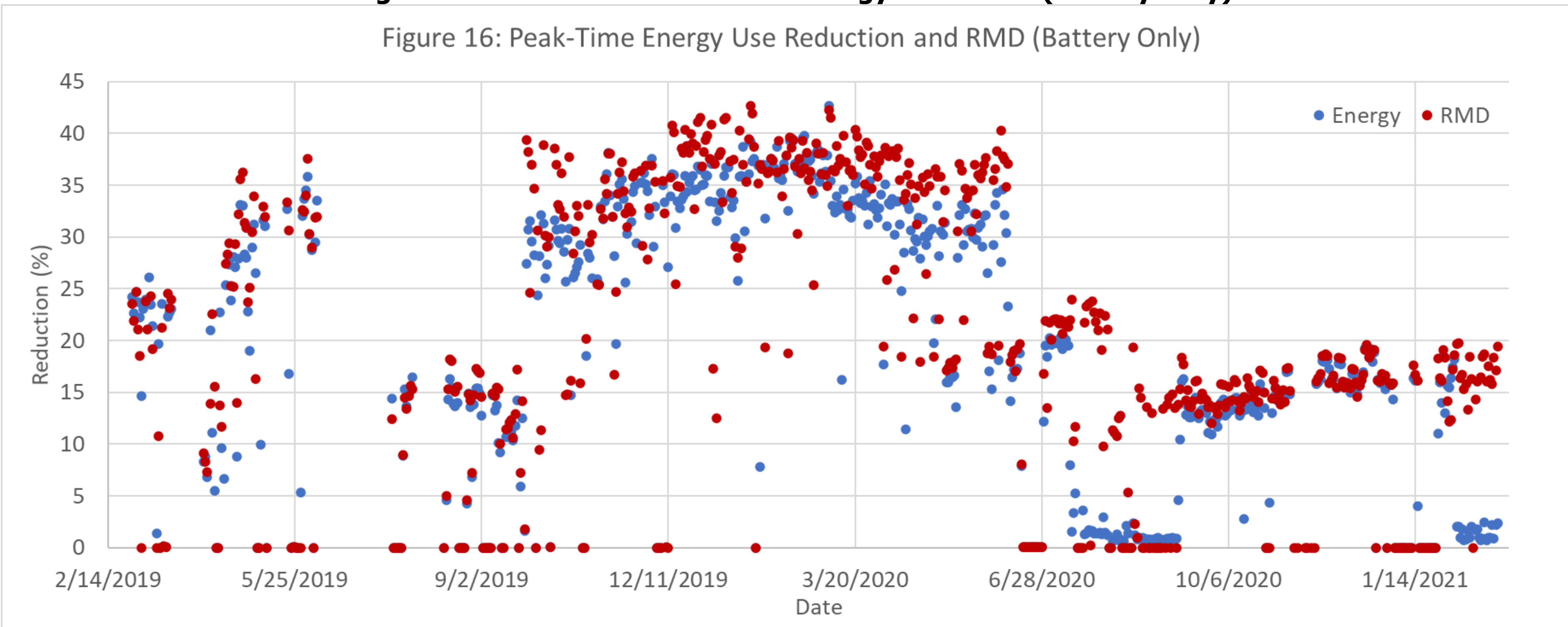

Reduction in maximum demand (RMD) and total peak time energy reduction provided by battery installation over 2 years.

Source: UC Davis

Other performance metrics were measured in addition to the site's overall peak-time energy reduction:

- Reduction in maximum demand (RMD) during peak hours: RMD was a proxy for quantifying demand charge management performance. This was defined as the reduction of the net demand compared to the demand at the time of maximum demand during peak hours.
- Highest microgrid performance (HMP): Another measure of demand reduction in terms of kW used was the maximum reduction in demand during peak hours, or HMP. This was distinct from RMD in that HMP considered the time during peak hours at which the reduction in demand was highest, rather than the reduction when the demand was highest. HMP and RMD are illustrated in Figure 13 and Figure 14, respectively. The mathematical definitions of the performance metrics are provided in Appendix A.
- Total energy usage reduction during peak hours: This was the primary measurement for determining if the microgrid met its goal of 10 percent to 60 percent reduction in peak-time energy use and measured the ability of the microgrid to perform peak shifting.

In the data in Figure 13, the ESS was able to reduce the maximum demand during peak hours by 19 percent with a standard deviation of 14 percent, with the highest reductions of 43 percent. The energy use during peak hours reduction was similar (average 18 percent with standard deviation of 13 percent).

The RMD performance results in Figure 13 and Figure 14 were low during the period from June 2019 to September 2019 because the battery was operating at 50 percent capacity. This reduction in capacity was due to a delay in replacing a failed safety relay. However, this demonstrated the importance of designing the two battery strings to be independent from one another, as the other string was able to continue operating while the first was being repaired. The similarly low results in 2020 were related to the COVID-19 pandemic, as one battery string required maintenance that could not be completed at the time due to COVID-19 related restrictions (such as limiting the number students on campus).

The data gaps seen in Figure 13 and Figure 14 for the spring and summer months of 2019 were caused by a failed hard drive in the PI server, in which performance data from March through September 2019 was corrupted. Fortunately, the information technology staff at UC Davis were able to recover about 60 percent of the data from the failed drive and restore it to a new drive. After this event, drives were setup in a redundant array of independent disks (commonly referred to as RAID) and regular backups were scheduled to prevent future data loss.

The goal for peak energy use reduction was 10 percent, with a stretch goal of 60 percent. While the stretch goal was not met, the system reduced the site's peak energy use by __ percent, more than double the original goal. Another goal was to demonstrate that the system could result in at least 10 percent electrical bill costs, which was achieved. The actual cost reduction depends on the billing tariff chosen, but was in the range of 10 percent to 15 percent based on tariff.

Figure 14: Total Power and Energy Reductions (2 Years)

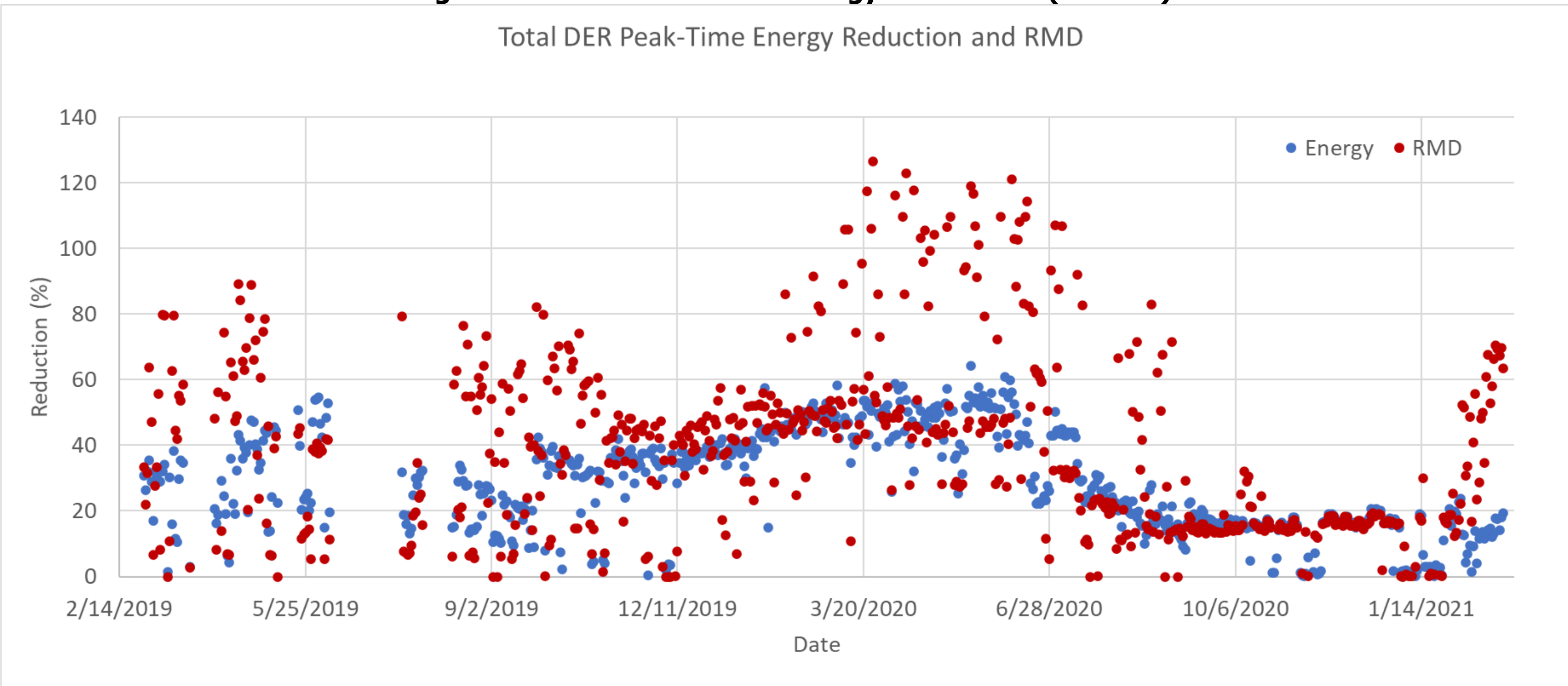

Scatter chart of reductions in peak-time energy use and RMD from solar PV paired with battery.

Source: UC Davis

Figure 15: Total Power and Energy Reductions (October 2019)

Plot of reductions in peak-time energy use and RMD from solar PV paired with battery. Plot shows zoomed in values from Figure 14 during the October 2019. "Power" refers to RMD, "Energy" refers to peak-time energy usage reduction.

Source: UC Davis

Figure 14 and Figure 15 show the reduction in peak power and energy usage when considering both solar and battery. The average reduction peak time energy use was 29 percent with a standard deviation of 15 percent, and the RMD was 38 percent with a standard deviation of 27 percent. The large variability in this figure is a result of the large quantity of PV installed at the site. Since the demand during peak hours is typically highest between 4 p.m. and 5 p.m. when PV generation is still a factor, the RMD during peak hours is largely a function of the season and the weather. This can be seen in Figure 14 between November 2019 and February 2020, which is the cloudy/rainy season in Davis, California. If it were not for the missing data during the summer and the reduced functionality of the battery, it is likely that the project would have met 60 percent stretch goal for RMD. Note, however, that the maximum value for RMD was 127 percent, more than double the stretch goal, and the stretch goal was met on 18 percent of days.

Figure 16 shows microgrid power data from December 17, 2019 from the microgrid with a 5-minute resolution. The "noisy" data is common on cloudy days and is caused by PV. There were nominally 200 kW of panels installed in the microgrid and the typical demand is only 80 kW, so a cloud passing overhead can cause a large disturbance to the net load of the grid. The net load and demand data were noisier than the PV data due to the resolution of the PV data being lower than that of the demand measurement. Note that negative battery power (grey dashed line) is charging and that the building demand (red) curve is a calculated value based on the other measured values in the plot.

$$Demand = Net\ Demand + PV + Battery$$

Figure 17 shows data from a sunny day where the data is much cleaner. Note that the spikes in the calculated demand persist due to misalignment of the data sources. It should also be noted that the PV (green) in Figure 16 and Figure 17 is for the pre-existing 120 kW PV array. The inverter for the newly added 80kW PV array did not report data to the data server. The plots data was manually downloaded from the PV inverters and added to the output of the existing PV array.

Figure 16: Microgrid Data, Cloudy Day (December 17, 2019)

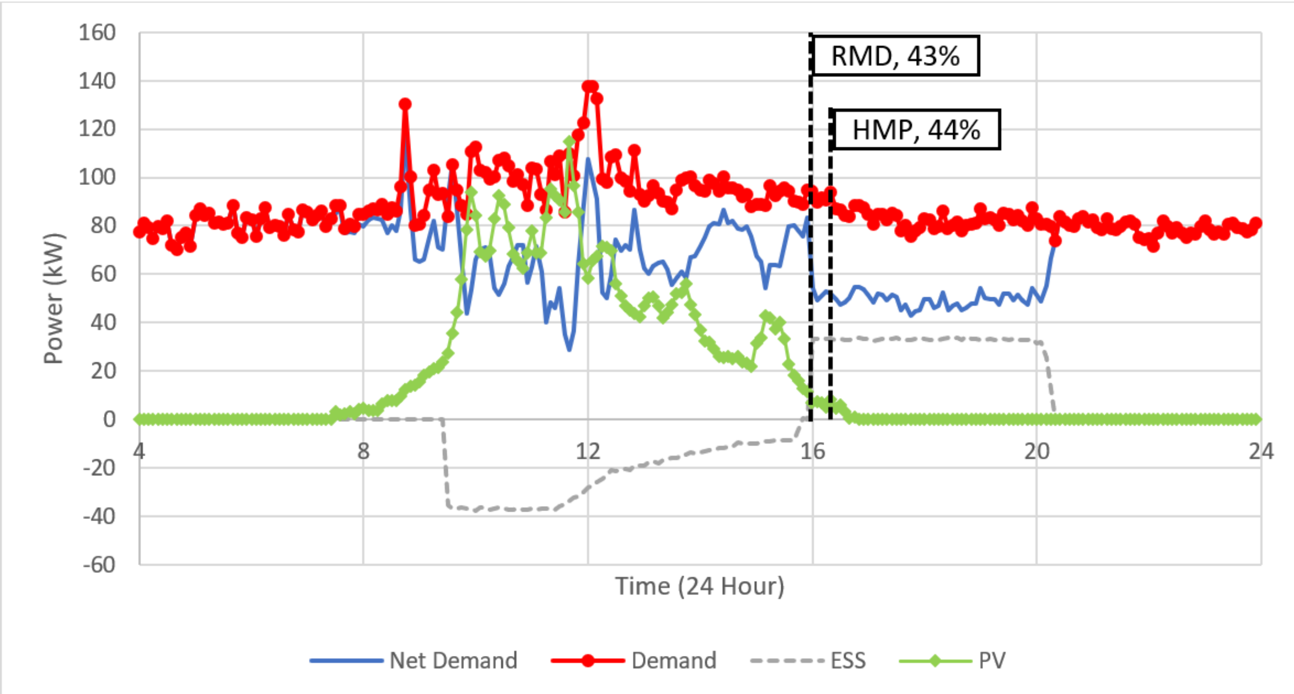

5-minute resolution power data from the microgrid showing operation during a cloudy day. Negative battery power indicates charging.

Source: UC Davis

Figure 17: Microgrid Data, Sunny Day (October 5, 2019)

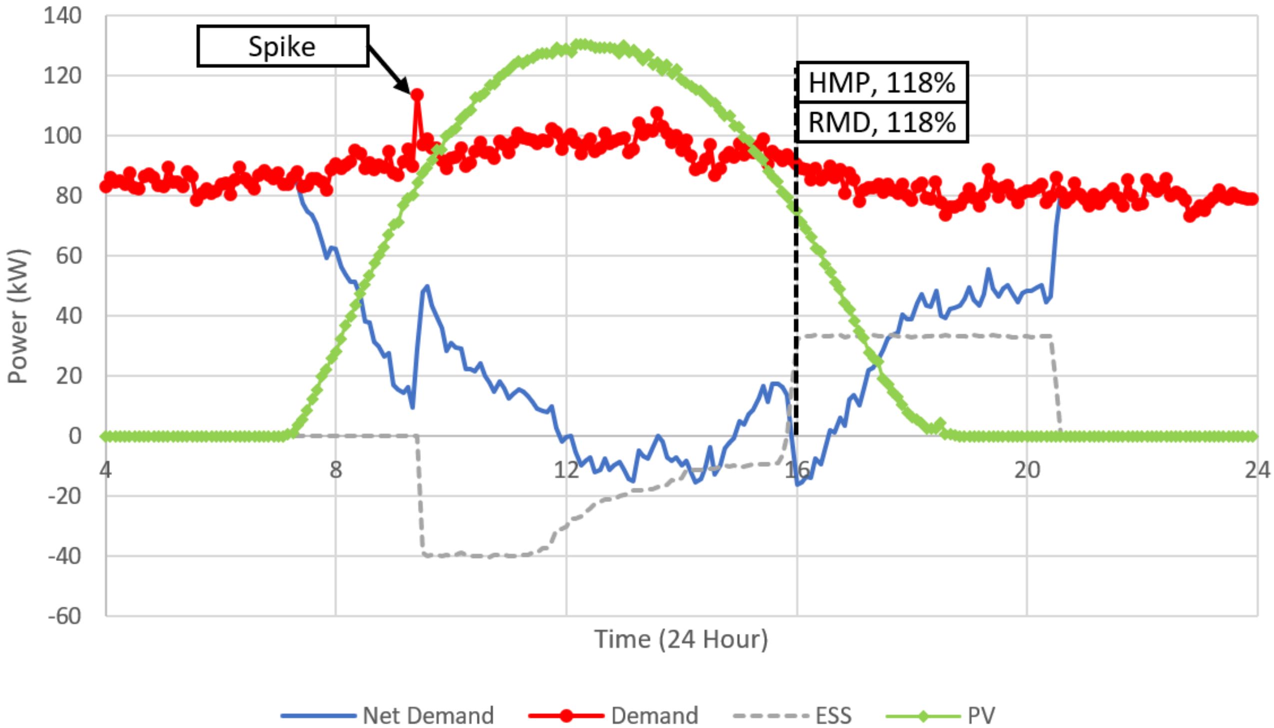

5-minute resolution power data from the microgrid October 5, 2019 showing operation during a sunny day. Negative battery power indicates charging. While it appears as if the HMP and RMD*??* is caused by the data misalignment spikes mentioned, this point was not immediately when the battery turned on. The point labeled "Spike" was caused by the battery shutting off, not an actual increase in demand, this would create a false measurement of RMD.

Source: UC Davis

The daily total charge and discharge energy of the battery is 155 kWh and 150kWh, respectively. This suggests that the round-trip efficiency of the battery is 97 percent, not including the inverter. Discharging 150 kWh/day from the battery is the equivalent of using 52 percent of the full capacity of the ESS. As mentioned earlier, the target DoD is 60 percent (20-80 percent SoC) which should be 172 kWh. The difference between the measured capacity of the ESS and the expected capacity based on the capacity of all the included battery modules comes from two sources: Poor SoC estimation by the BMS and calendar aging of the battery modules. The Orion BMS calculates SoC using current integration and corrections based on cell voltages. Unfortunately, the ripple current from the inverter that can be seen in Figure 16 and Figure 17 affected the BMS's ability to properly calculate the SoC of the battery.

Figure 18: Daily Reduction in Maximum Demand (2 years)

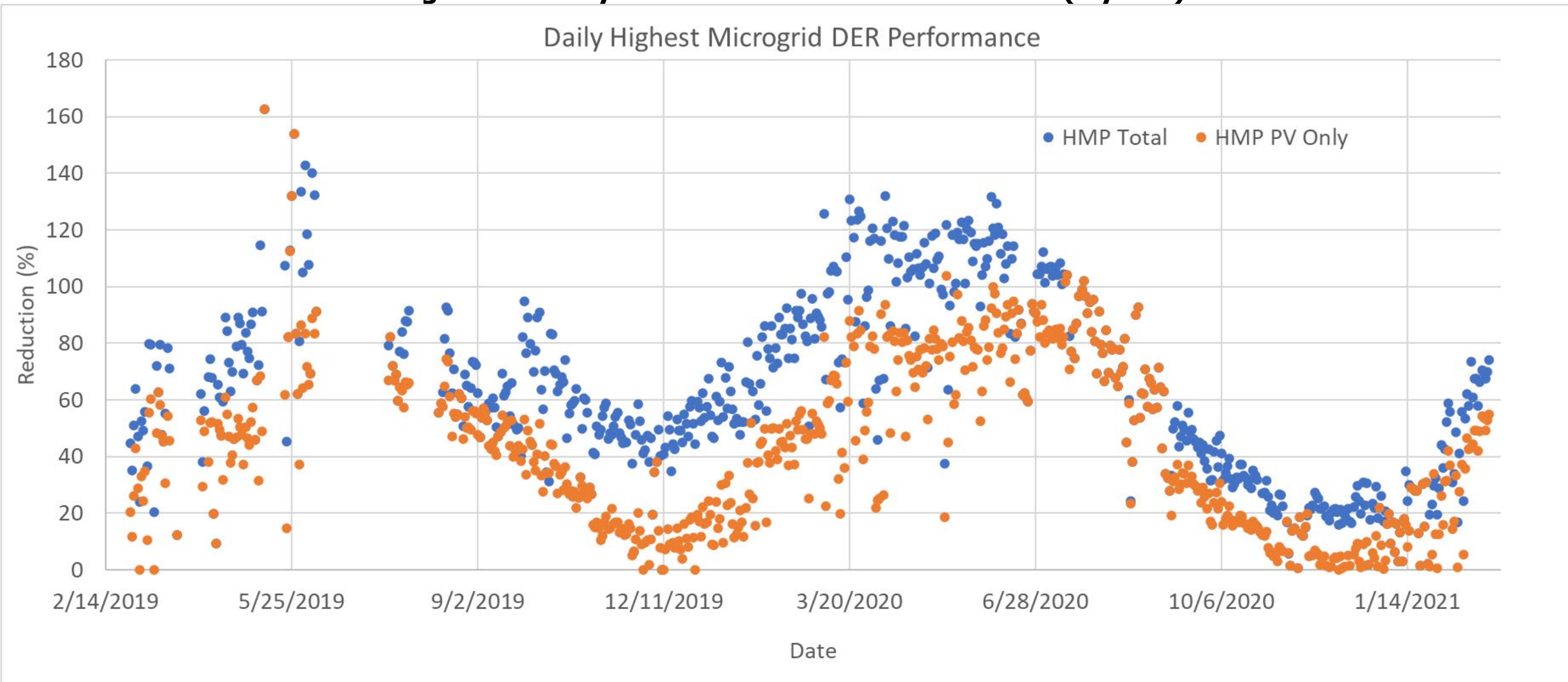

Highest Microgrid Performance (HMP) during peak hours showing the difference between PV only and PV+ESS installed in the microgrid.

Source: UC Davis

Figure 18 shows that the performance of the microgrid was highly seasonal, as would be expected thanks to the large amount of installed PV. Note that HMP is the highest percent of demand that was met by renewables on each day and typically occurs early during peak hours when solar generation is still significant but decreasing. During summer, PV contributes the most to HMP, but during the winter, the battery is essential in preserving microgrid performance.

One unaccomplished goal was the demonstration of autonomous frequency and voltage control to mitigate grid stability issues. This was not completed for two reasons. First, the project partner at OSIsoft who was to implement this section of the controller chose not to participate in the project. Second, due to a change of selection for the battery inverter due to cost and supply constraints, the inverter could not perform these functions.

A related objective not completed was reducing the SAIDI by at least 50 percent. Unfortunately, the UC Davis facilities group was not interested in this functionality for the system being installed, claiming that the UC Davis grid already has a SAIDI of zero for many of its buildings. They, along with the fire department, were also not interested in parts of the system being powered during a power outage due to concerns that some systems may still be energized during repairs on the distribution system or fire suppression activities. Therefore, the researchers were required to shut the system down during power outages, disrupting any demonstration on the potential resiliency benefits of the system.

Another objective that the team was unable to complete was demonstration of selling ancillary services to California ISO. This project was too small to qualify for participation, and the administrative hurdles required, even with a sufficiently large system, were too high for the small project team to deal with. It was also likely that participating in California ISO’s ancillary services market could have limited the flexibility of testing other energy management modes and limited this project’s usefulness as a research platform.

System Simulation Results

The benefits of the microgrid were estimated using the Matlab simulation described in Chapter 2.

Reductions in GHG emissions were based on increased installation of solar PV at the site as well as increased solar self-consumption from storing overgeneration in the batteries for later use. When not considering storage of PV energy in the battery, the simulation (discussed below) did not provide CO_2 reduction credit for any over-generation sent to the grid. Therefore, by storing PV energy in the battery the system’s CO_2 footprint was reduced. Using the average of 0.215 kg CO_2/kWh from the United States Energy Information Administration (U.S. Energy Information Administration, 2014), and the total annual energy generation from the PV arrays, the reduction is 62 metric tons/year, or a 40 percent reduction. GHG savings would be larger if the real-time carbon-intensity of the California grid were considered. This is because in the evening when solar power begins to fade, the least efficient peaker power plants are used to meet the demand. This is the period when the battery is discharged, potentially offsetting significantly more carbon than using the average CO_2/kWh figure for California would suggest.

Carbon footprint reduction were highest in July and lowest in December due to more limited PV generation. The total reduction in carbon footprint was calculated to be 10 percent, or 14,000 kg CO_2. If the simulation considered real-time grid electricity carbon intensity, which is available for California from the California ISO (California ISO, 2019), the microgrid would likely reduce the carbon footprint even further, as seen in Figure 23 in Chapter 6. Because the simulation currently calculates CO_2 reductions, carbon credits are not provided for over-generation of PV. This allows the battery to realize some CO_2 reduction, but if real-time data were used, the battery could be optimized to charge when the grid had the lowest CO_2 emissions rate which is during the day due to the large amount of solar generation in California.

Peak demand was significantly reduced (**Figure** 20) due to the peak shaving capability of the battery, in some cases reducing peak demand by 40 percent. The average reduction in peak-time demand was 31 percent, with a standard deviation of 12 percent. The peak reduction showed a strong dependence on the month due to the changes in PV production.

Figure 19: Microgrid Simulation Results

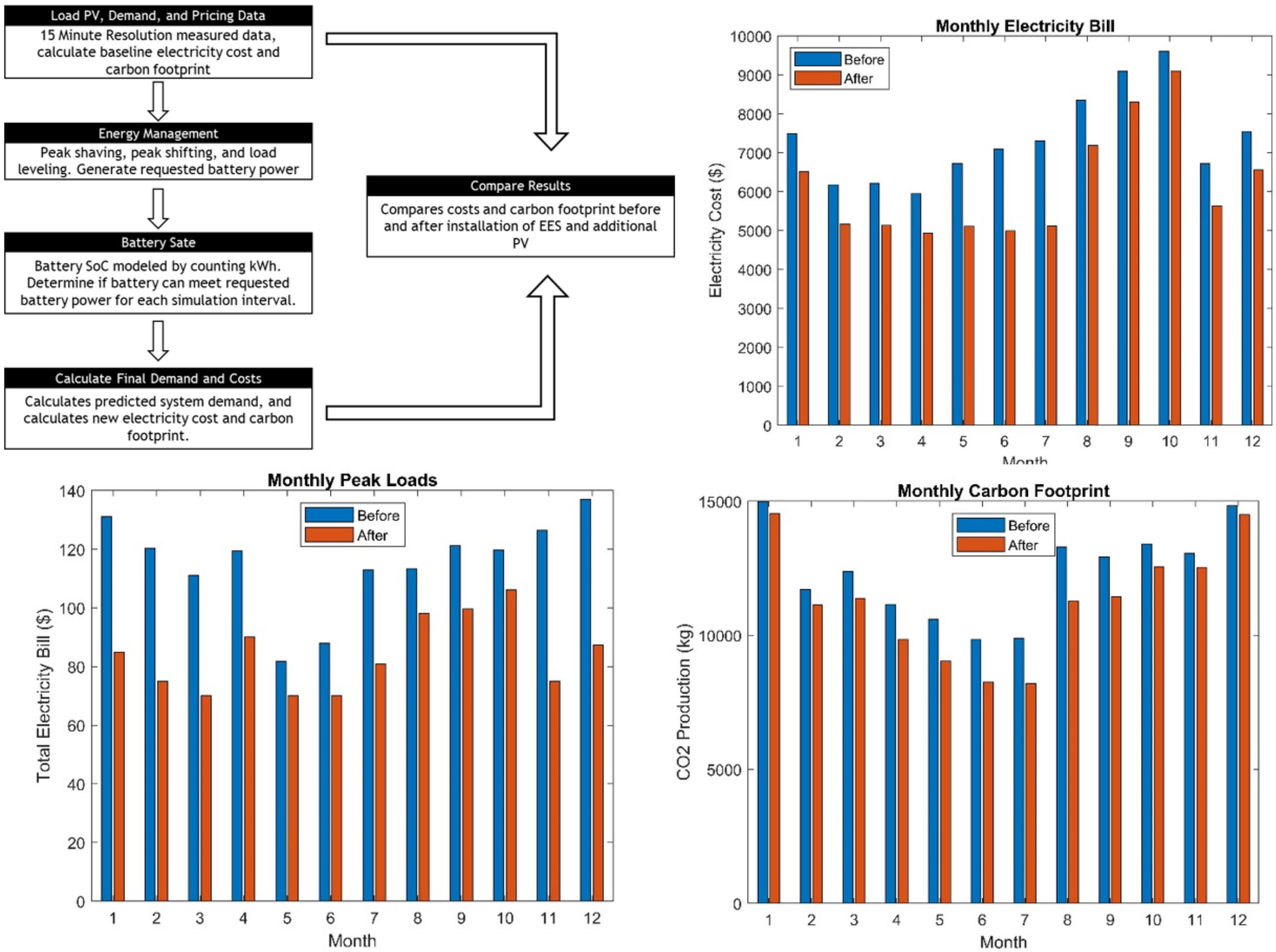

Top Left: Functional diagram of simulation steps. Top Right: Simulated monthly electricity bill savings. Bottom Left: Simulated reduction in monthly peak loads. Bottom Right: Simulated reduction in monthly carbon footprint of the microgrid.

Source: UC Davis

Figure 20: Maximum Peak Demand Reduction

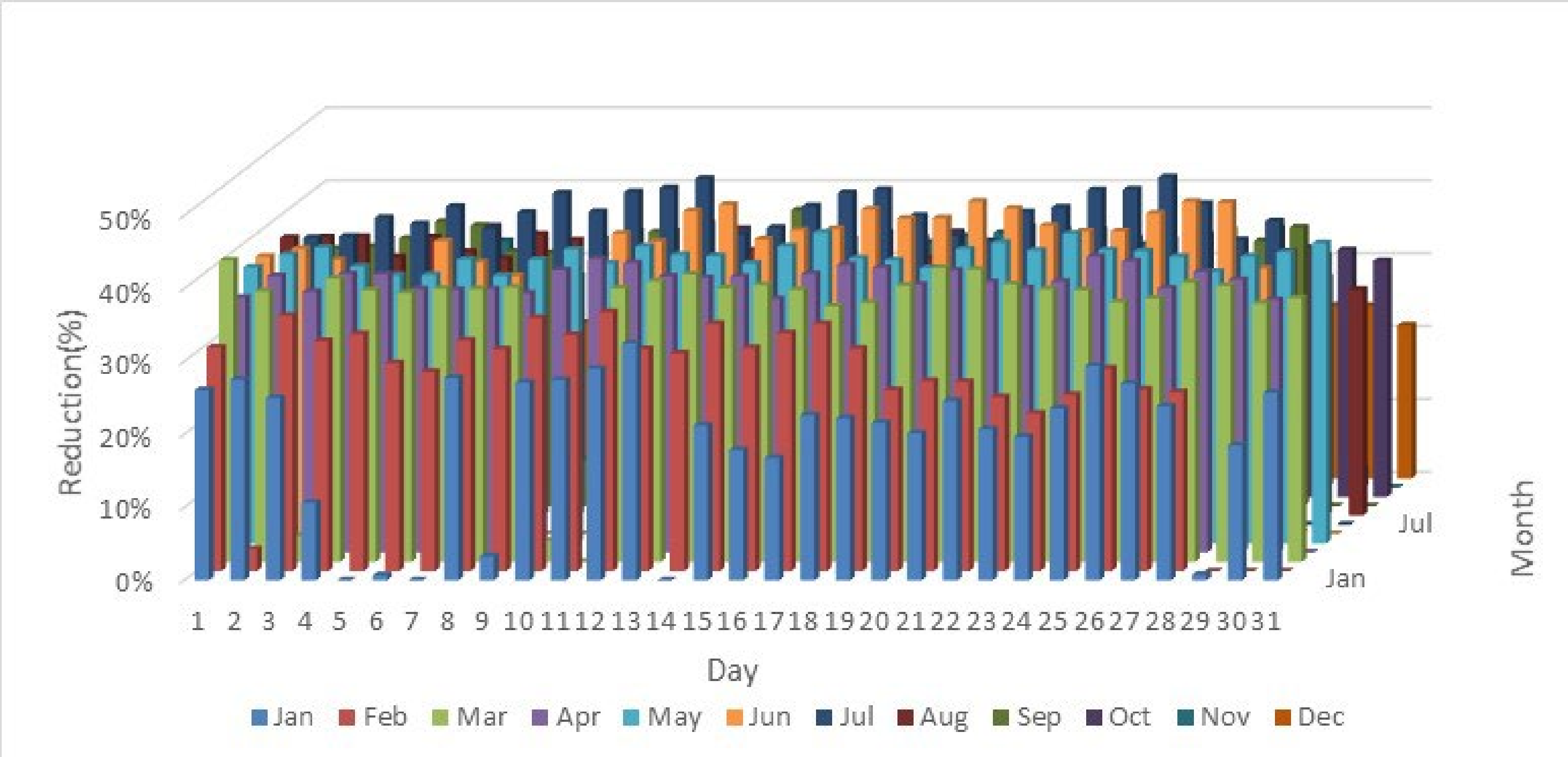

Simulated daily peak-time maximum demand reduction

Source: UC Davis

The peak-time energy usage was reduced (Figure 21) due to the battery operating in peak shifting mode. The average reduction in peak-time energy use was 33 percent with a standard deviation of 14 percent. The maximum reduction in peak-time energy use was 64 percent. As with the peak-time maximum demand, the peak-time energy use was also seasonally dependent due to the changes in PV production. The total reduction in energy demand of the whole microgrid was 11 percent over one year. As a result, the simulation predicts that the microgrid will save $12,000 per year, a 14 percent reduction is electricity costs, compared to not having a microgrid.

CHAPTER 4: Technology/Knowledge/Market Transfer Activities

Principal Investigator Professor Park's laboratory has posted information about the project on the lab's website at https://research.engineering.ucdavis.edu/greentech/bwf-microgrid/. The laboratory has also placed flyers around the UC Davis campus advertising this project, which was successful in bringing more than 20 students to work on the project in the lab. This gave the students valuable experience on an actual project to supplement their classroom education. A research paper is in the process of being submitted at the time of this report's writing with the working title of "Development and Demonstration of Microgrid System Utilizing Second-Life EV Batteries".

Based on experience from this project, the UC Davis research team started a company, RePurpose Energy[9] to commercialize and further develop the technology from this project. Initial markets include medium sized ESSs to pair with commercial and industrial solar installations. The market for this type of energy storage is expected to reach nearly $1B by 2024 (Wood Mackenzie Power & Renewables, 2019). In addition, UC Davis has made the microgrid and battery system part of their tour for groups visiting the various energy efficiency related research organizations at UC Davis.

This demonstration project stimulates the market for second-life battery systems by addressing various industry concerns with second-life batteries such as cell performance and reliability, and safety in a large-scale ESS. This project demonstrated that second-life batteries are perfectly capable of performing peak-shifting. While the ESS overall had reliability issues as described above, none of these issues were due to the battery cells themselves, showing that these cells installed in a more refined ESS would result in highly reliable performance. While still having run for only a relatively short time, no safety issues arose in the system, also showing that second-life batteries can be operated safely for microgrid usage.

that

Partial List of Visitors and Tours of the Microgrid

- David Hochschild, Chair of the California Energy Commission
- Cecilia Aguiar-Curry, Yolo County California Assembly Member
- Jared Blumenfeld, CalEPA Secretary for Environmental Protection
- Delegation from Panasonic
- Phil Hopkins, Wells Fargo
- Dr. Wendy Fong, Professor at Lehigh University and director of Industry Engage
- High school students participating UC Davis SMASH and COSMOS Programs

[9] www.repurpose.energy

- Takeyuki Yamaki, Chief Technology Officer for Panasonic
- Fujita Corp representatives
- SMUD representatives
- California Public Utilities Commission
- Gary Simon, Chairman, Clean Start
- Jill Anderson, Vice President of Customer Programs and Services, Southern California Edison

Figure 21: California Energy Commission Members Visit the Microgrid

Photo from the California Energy Commission's site visit on March 5, 2019.

Source: California Energy Commission's Photostream, Flickr.

CHAPTER 5: Conclusions and Recommendations

A microgrid ESS was designed and built using second-life Nissan LEAF battery modules. The battery modules were tested and found to have an average SoH of 77.8 percent. The test data was used to sort the modules such that they were matched together for parallel connection with modules that had as similar resistance as possible to prolong the cycle life. Comparison of the modules used in the microgrid to spare modules showed that degradation of the used cells was not faster than calendar aging of the stored cells.

The selection of power conversion equipment for battery systems of this size was limited, resulting in a high price and long lead times. The CEC may wish to consider promoting the development of new inverter technologies for microgrids and battery systems to increase competition in this space. For example, inverters with lower DC current ripple, modular architecture so that they can be used in systems designed for single buildings or whole microgrids, or wide DC voltage input ranges for increased battery compatibility. This would result in the installed cost of ESSs, especially smaller systems, being significantly reduced.

A simulation of the microgrid performance was developed to estimate the economic benefits of installing the system, and it was found that the system could save up to $12,000 per year compared to before it was installed. Real operational data was also presented, showing the reduction in peak-time energy and power demand of 30 percent to 40 percent compared to the project goal of 10 percent. Data was also shown for operation on sunny days with abundant solar generation and cloudy days with highly intermittent solar generation.

Thus far, the second-life battery cells themselves have performed as expected, and in fact have been the most reliable component of the microgrid along with the solar PV as compared to the downtime caused by other component failures. This may be in part due to the ‘gentle’ usage profile that was chosen to maximize their lifetime but is also a reasonable use case for stationary energy storage. Therefore, for at some load profiles, the use of second-life cells for ESS is perfectly viable.

One great hurdle to commercial deployment of second-life batteries is the subsidies for new batteries that are not equally available to second-life batteries. California’s Self-Generation Incentive Program explicitly excludes second-life batteries from receiving incentives but provides a substantial subsidy for new batteries that makes them nearly free. This runs counter to the goals of GHG emissions because it incentivizes production of more lithium-ion battery cells from newly mined materials, which is a potentially environmentally destructive process.[10] [11] [12] [13] [14]

[10] K. Richa, C.W. Babbitt, N.G. Nenadic, G. Gaustad, Environmental trade-offs across cascading lithium-ion battery life cycles, The International Journal of Life Cycle Assessment 22 (1) (2017) 66–81.

[11] R. Sathre, C.D. Scown, O. Kavvada, T.P. Hendrickson, Energy and climate effects of second-life use of electric vehicle batteries in California through 2050, Journal of Power Sources 288 (2015) 82–91.

[12] J.F. Peters, M. Baumann, B. Zimmermann, J. Braun, M. Weil, The environmental impact of Li-Ion batteries and the role of key parameters – A review, Renewable and Sustainable Energy Reviews 67 (2017) 491–506.

[13] Amnesty International, "This is what We Die For": Human Rights Abuses in the Democratic Republic of the Congo Power the Global Trade in Cobalt, Amnesty International (2016).

[14] U.S. Bureau of Land Management and U.S. Fish and Wildlife Service, *Thacker Pass Lithium Mine Project: Draft Environmental Impact Statement* (2020).

CHAPTER 6: Benefits to Ratepayers

Helping to Meet California's Energy and Environmental Goals

The microgrid provides the three primary benefits of the technology, as documented in the CEC report, *Microgrid Assessment and Recommendations to Guide Future Investments* (July 2015):

1. Reliability benefits by increasing the reliability of local loads.
2. Economic benefits by lowering facility costs.
3. Sustainability benefits from reducing GHG emissions

Realization of these benefits directly affects and improves California's ability to meet its statutory energy and environmental goals. In particular, the project has reduced the GHG emissions from the site's energy demand as mandated under Assembly Bill 32 (Nunez, Chapter 488, Statutes of 2006). The project increased the share of the facility's power derived from renewables, bringing down energy costs and carbon emissions. This project presents a path to reduce carbon emissions due to reduced reliance on the traditional fossil-fuel generation and energy-efficiency improvements.

With respect to grid reliability and economic benefits, the project contributed directly to the state's goals under Assembly Bill 2514 (Skinner, Chapter 469, Statutes of 2010). This bill requires utilities to examine and increase their use of energy storage and renewable energy over the next 10 to 15 years. The use, and demonstration of the feasibility, of second-life batteries brings down the cost of implementing energy storage technologies. Therefore, in addition to providing critical energy resources to the community, the microgrid provides a solution for increasing the penetration of renewable energy into the California grid without sacrificing grid stability and reliability.

To aid in California's goal of moving the electrical grid to renewable energy while also increasing its reliability and security, a large number of microgrids with a varied portfolio of DERs will be required. Installation of a microgrid makes the attached loads less reliant on the utility grid, meaning they have increased availability. The microgrid's ESS prevents back-feeding to the grid while also reducing peak demands, thus alleviating strain on the utility grid caused by solar over-generation and EV charging demands. By installing PV panels and ESS, the system significantly decreases the carbon-intensity of its consumed electricity.

This will also reduce the valley in the California ISO "duck curve", by not exporting excess solar power to the grid during peak solar generation. Then, during peak load hours, the ESS can be discharged to reduce the required ramp-rate of generating stations on the primary grid. This method of energy management could result in greater reliability for the grid, lower costs for consumers, and increased safety during grid power failure if deployed widely.

Quantitative Benefits

The project team calculated energy, demand, and cost benefits for the system based on measured values and simulation.

1. The 200-kW solar system generates **292 MWh** of energy per year. Using a $0.156/kWh electricity price, the annual value of generated electricity is approximately **$45,500** per year.
2. The generated solar electricity reduces GHG emissions by **56 metric tons** of CO_2 per year. Considering the current demand of the microgrid of **726 MWh/yr.**, the carbon footprint has been reduced by **40 percent**.
3. Based on California's power generation portfolio, the microgrid will lead to **6 metric tons** of avoided NOx emissions.
4. The 60 kW ESS reduces peak time demand by **26 percent to 40 percent**. The ESS has the potential to eliminate demand charges of up to **$38,000 per year** in the best-case scenario, with **$25,000** more likely. This assumes $18/kW for demand charges.
5. Theoretical ability to provide up to 4 hours of backup power

Analysis of the backup power capability of the system was done in Matlab based on a year of operational data. The plot in Figure 22 uses the average demand (~80kW) of the building, and scales that based on the shown critical load percent. The resiliency calculations include PV generation, so if an outage were to occur at night, resiliency would be lower than shown in the plot. Considering the daily average *net* load of the microgrid (demand – PV generation), the ESS would be capable of meeting a 4-hour resiliency requirement on 93 percent of days with no DR or load reduction.

Figure 22: Simulated Backup Power Capability of Energy Storage System

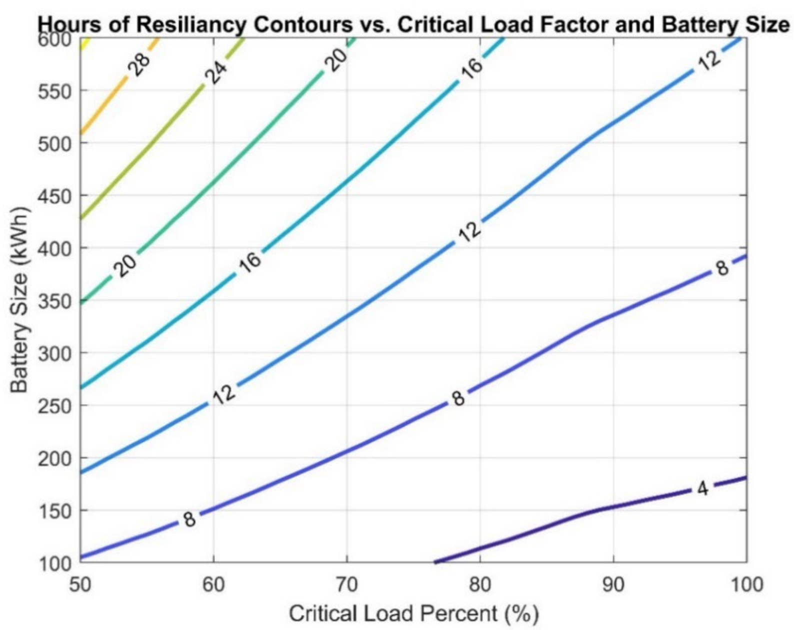

Contour plot showing how critical load factor and battery size affect backup power capability of the site. Numbers on the contour lines represent the number of hours the microgrid could run without a grid connection.

Source: UC Davis

CO_2 savings were due primarily to the reduction in purchased electricity from the grid due to onsite PV. However, additional CO_2 savings are expected due to the variability of the renewable generation fraction of the California grid due to solar. Thus, by purchasing electricity during the day from the utility grid and using PV energy stored in the ESS during the evening and night, the CO_2 footprint of the microgrid can see additional reductions. For example, consider January 8, 2020 in Figure 23 which shows the carbon emissions in metric tons of CO_2/MWh for California ISO's electricity supply. During the day, when solar production is highest (note that January 8, 2020 was a cloudy day in Northern California), the carbon intensity of the grid is more than 30 percent lower than at night.

Figure 23: California ISO Grid Carbon Intensity

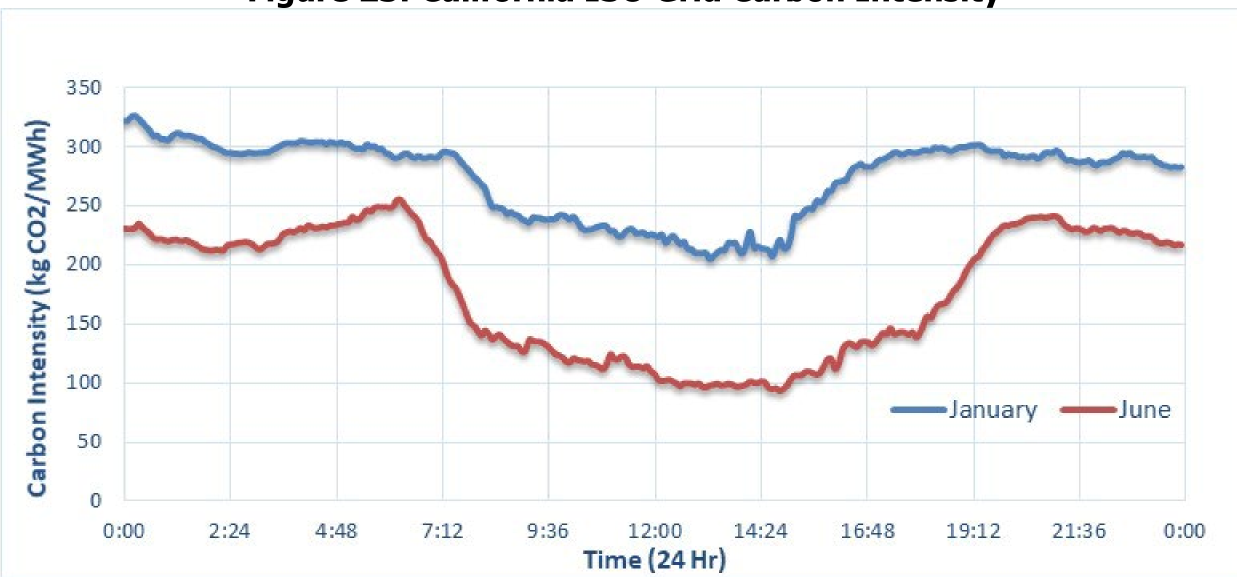

Carbon intensity for California ISO generation on January 8, 2020 compared to June 7, 2019. (California ISO, 2019)

Source: Data from California ISO. Figure generated by UC Davis.

Figure 24 shows the load of the microgrid before and after the installation of new PV and ESS. Before system installation, the microgrid contributed to the duck curve due to the already installed PV. After installing additional PV and the ESS, the PV is used to charge the battery during the day (point A), limiting over-generation and mitigating the grid's overall need to curtail solar generation. Even when charging the battery, the net load still shows a reduction compared to before the system was installed. In the evening during peak hours and when PV production starts to decline, the battery begins to discharge (point B). This maintains the netload of the microgrid well below its previous value during peak hours and reduces the slope of the duck curve's high evening ramp rate. After peak hours, the battery stops discharging (point C), and the microgrid's demand returns to its nominal value. By also implementing peak-shaving (which the ESS is capable of, but is not in its current operating mode), it is also possible to eliminate demand spikes which then avoids large demand charges. This mode would provide even greater economic benefits for the microgrid owner as demand charges can be a large portion of an energy bill for some customers. In turn, the increased economic benefits increase the incentive to install more energy storage, which benefits the California grid further through increase resiliency and reduced peak demand.

California stands to gain much by large scale adoption of second-life battery ESSs. These systems can provide the same grid benefits of new batteries, but at reduced cost. Lower cost can lead to increased deployment and thus total installed capacity. This opens opportunities for advanced grid management strategies by integration of large ESSs with California ISO to help limit power outages, or to defer certain electrical system upgrades by, for example, using batteries to keep local demand under the capacity of a local substation. Finally, since California is home to most of the nation's EVs, it has a first mover advantage in the second-life energy storage industry. Shipping lithium-ion batteries is expensive and incurs regulatory costs, so it is good strategy for second-life ESS manufactures to set up shop in California, where the supply of EVs and their batteries is high. Then, when the rest of the country catches up, the industry will have already been established in California, making it the leader in this technology.

Figure 24: Microgrid Demand Before and After

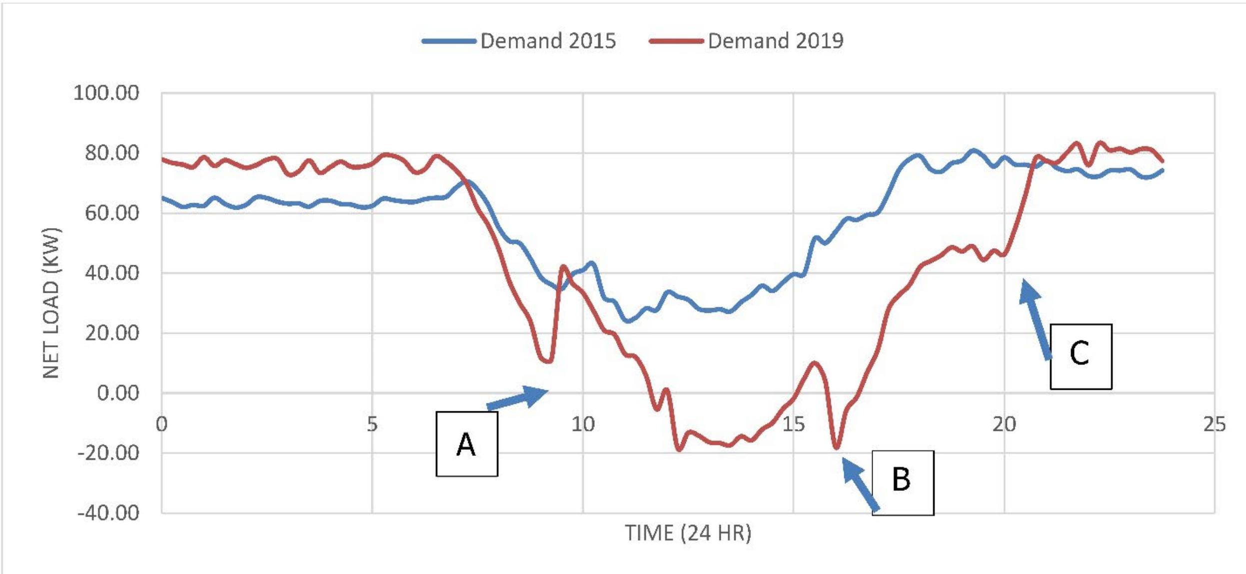

Microgrid load data before and after system installation. Data for October 6, 2015 and October 6, 2019.

Source: UC Davis

LIST OF ACRONYMS

Term	Definition
A	Amp
AC	Alternating Current
BMS	Battery Management System
California ISO	California Independent System Operator
CEC	California Energy Commission
CO_2	Carbon Dioxide
CPCV	Constant Power, Constant Voltage
DC	Direct Current
DER	Distributed Energy Resource
DR	Demand Response
ESS	Energy Storage System
EMS	Energy Management System
EPIC	Electric Program Investment Charge
EPO	Emergency Power Off
EV	Electric Vehicle
GHG	Greenhouse Gas
GWh	Gigawatt-Hour
HMP	Highest Microgrid Performance
kg	Kilogram
kW	Kilowatt
kWh	Kilowatt-Hour
LEED	Leadership in Energy and Environmental Design
MW	Megawatt
MWh	Megawatt-Hour
NREL	National Renewable Energy Laboratory
PI	Plant Information
PV	Photovoltaic
RMD	Reduction in Maximum Demand

Term	Definition
RMI	Robert Mondavi Institute
SAIDI	System Average Interruption Duration Index
SoC	State of Charge: amount of energy remaining in the battery
SoH	State of Health: level of battery degradation in the battery
UC	University of California
V	Volt

REFERENCES

California Independent System Operator. (2019). *Today's Outlook*. Retrieved 8 19, 2019, from http://www.caiso.com/TodaysOutlook/Pages/emissions.aspx

Conway, J. (2019, 8 6). *Total number of wineries in the United States from 2009 to 2019*. Retrieved 1 14, 2020, from Statista: https://www.statista.com/statistics/259353/number-of-wineries-in-the-us/

Debnath, U. K., Ahmad, I., & Habibi, D. (2014). Quantifying economic benefits of second life batteries of gridablevehicles in the smart grid. *Electrical Power and Energy Systems, 63*, 577-587.

Discover California Wines. (2018). *Statistics*. Retrieved 1 14, 2020, from Discover California Wines: https://discovercaliforniawines.com/media-trade/statistics/

Gogoana, R., Pinson, M. B., Bazant, M. Z., & Sarma, S. (2014). Internal resistance matching for parallel-connected lithium-ion cells and impacts on battery pack cycle life. *Journal of Power Sources, 252*, 8-13.

National Renewable Energy Laboratory. (2017, August). *PVWatts Calculator*. (Alliance for Sustainable Energy) Retrieved 4 13, 2018, from https://pvwatts.nrel.gov/

Pacific Gas & Electric Company. (2018). *Time-of-Use Rate Plans*. Retrieved 11 3, 2019, from https://www.pge.com/en_US/residential/rate-plans/rate-plan-options/time-of-use-base-plan/time-of-use-plan.page

Pacific Gas and Electric Company. (n.d.). *Tariffs*. Retrieved 7 20, 2018, from https://www.pge.com/tariffs/index.page

Saxena, S., Le Floch, C., MacDonald, J., & Moura, S. (2015). Quantifying EV battery end-of-life through analysis of travel needs with vehicle powertrain models. *Journal of Power Sources, 282*, 265-276.

Saxena, S., MacDonald, J., & Moura, S. (2015). Charging ahead on the transition to electric vehicles with standard 120 V wall outlets. *Applied Energy, 157*, 720-728.

U.S. Energy Information Administration. (2014). *Electrity: State Electricity Profiles*. Retrieved 11 4, 2019, from https://www.eia.gov/electricity/state/archive/2014/california/

UC Davis Facilities Management Energy Conservation Office. (2020, 1 14). *Robert Mondavi Institute*. Retrieved from CEED: https://ceed.ucdavis.edu/

Wines & Vines. (2014, 1 27). *Number of Wineries Grows to 8,391 in North America*. Retrieved 1 14, 2020, from Wines Vines Analytics: https://winesvinesanalytics.com/news/article/127266/Number-of-Wineries-Grows-to-8391-in-North-America

Wood Mackenzie Power & Renewables. (2019). *U.S. Energy Storage Monitor.* Washington DC: Energy Storage Association.

APPENDIX A: Microgrid Performance Metric Equations

Peak-Time Energy Use Reduction

The reduction in energy use during peak hours was defined as:

$$Reduction_{kWh}(\%) = \frac{\int_{4PM}^{9PM}(P_{demand_t} - P_{net_t})dt}{\int_{4PM}^{9PM} P_{demand_t} dt} \times 100\% \quad (1)$$

Where P_{demand} is the total electricity demand in kW of the microgrid, t is the time evaluated between 4:00 PM and 9:00 PM for peak hours, and P_{net} is the measured power in kW at the point of common coupling with the university grid.

Reduction in Maximum Demand

The reduction in maximum demand (RMD) during peak hours was defined as:

$$RMD_{kW}(\%) = \frac{P_{demand_t} - P_{net_t}}{P_{demand_t}} \times 100\% \quad \Big|_{t=t(\max(P_{demand}))} \quad (2)$$

Highest Microgrid Performance

The highest microgrid performance (HMP) during peak hours was defined as:

$$HMP_{kW}(\%) = \frac{\max(P_{demand_t} - P_{net_t})}{\mathrm{P_{demand_t}}} \times 100\% \quad (3)$$